# Accepted Manuscript

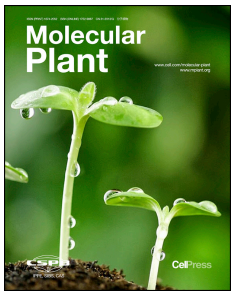


A *Phytophthora capsici* RXLR Effector Targets and Inhibits a Plant PPIase to Suppress Endoplasmic Reticulum-Mediated Immunity

Guangjin Fan, Yang Yang, Tingting Li, Wenqin Lu, Yu Du, Xiaoyu Qiang, Qujiang Wen, Weixing Shan

PII: S1674-2052(18)30186-2
DOI: 10.1016/j.molp.2018.05.009
Reference: MOLP 634

To appear in: *MOLECULAR PLANT*
Accepted Date: 27 May 2018

Please cite this article as: **Fan G., Yang Y., Li T., Lu W., Du Y., Qiang X., Wen Q., and Shan W.** (2018). A *Phytophthora capsici* RXLR Effector Targets and Inhibits a Plant PPIase to Suppress Endoplasmic Reticulum-Mediated Immunity. Mol. Plant. doi: 10.1016/j.molp.2018.05.009.

# A *Phytophthora capsici* RXLR Effector Targets and Inhibits a Plant PPIase to Suppress Endoplasmic Reticulum-Mediated Immunity

Guangjin Fan[1], Yang Yang[2], Tingting Li[2], Wenqin Lu[1], Yu Du[3], Xiaoyu Qiang[2], Qujiang Wen[1], and Weixing Shan[2*]

[1] State Key Laboratory of Crop Stress Biology for Arid Areas and College of Plant Protection, Northwest A&F University, Yangling, Shaanxi 712100, China;

[2] State Key Laboratory of Crop Stress Biology for Arid Areas and College of Agronomy, Northwest A&F University, Yangling, Shaanxi 712100, China;

[3] State Key Laboratory of Crop Stress Biology for Arid Areas and College of Horticulture, Northwest A&F University, Yangling, Shaanxi 712100, China.

* Correspondence: Weixing Shan (E-mail: wxshan@nwafu.edu.cn).

Running title: PcAvr3a12 Targets and Inhibits a Plant PPIase

Short Summary:

*Phytophthora* pathogens secrete numerous effectors that manipulate host processes to induce plant susceptibility. *P. capsici* deploys a virulence RXLR effector, PcAvr3a12, a member of Avr3a family, to facilitate infection by targeting and suppressing around haustoria a novel Endoplasmic Reticulum (ER)-localized PPIase, AtFKBP15-2, which is involved in ER-stress sensing and ER-stress mediated plant immunity.

## ABSTRACT

*Phytophthora* pathogens secrete a large arsenal of effectors that manipulate host processes to create an environment conducive to their colonization. However, the underlying mechanisms by which *Phytophthora* effectors manipulate host plant cells still remain largely unclear. In this study, we report that PcAvr3a12, a *Phytophthora capsici* RXLR effector and a member of the Avr3a effector family, suppresses plant immunity by targeting and inhibiting peptidyl-prolyl *cis-trans* isomerase (PPIase). Overexpression of *PcAvr3a12* in *Arabidopsis thaliana* enhanced plant susceptibility to *P. capsici*. FKBP15-2, an endoplasmic reticulum (ER) localized protein, was identified as a host target of PcAvr3a12 during early *P. capsici* infection. Analyses of *A. thaliana* T-DNA insertion mutant (*fkbp15-2*), RNAi and overexpression lines consistently showed that FKBP15-2 positively regulates plant immunity in response to *Phytophthora* infection. FKBP15-2 possesses PPIase activity essential for its contribution to immunity but was directly suppressed by PcAvr3a12. Interestingly, we found that FKBP15-2 is involved in ER stress sensing and is required for ER stress-mediated plant immunity. Taken together, these results suggest that *P. capsici* deploys an RXLR effector, PcAvr3a12, to facilitate infection by targeting and suppressing a novel ER-localized PPIase, FKBP15-2, which is required for ER stress-mediated plant immunity.


**Key words:** RXLR effector; Avr3a; FKBP; ER stress; immunity; *Phytophthora capsici*

## INTRODUCTION

Plants have evolved multiple complex signal transduction pathways to synergistically respond to pathogen threats. These responses are conferred by a two-layered innate immune system, consisting of pattern-triggered immunity (PTI) and effector-triggered immunity (ETI) (Jones and Dangl, 2006; Dodds and Rathjen, 2010). These innate immune systems often rely on basic cellular processes to defend against pathogens, such as the endoplasmic reticulum (ER) quality control system (Li et al., 2009) and hormone signaling (Kazan and Lyons, 2014). However, successful plant pathogens can secrete a plethora of effectors to interfere with many host cellular processes in order to establish colonization (Dou and Zhou, 2012; Qiao et al., 2013; Turnbull et al., 2017). Thus, insights into effector targets and target functions reveal both pathogen infection mechanisms and novel plant components of immunity.

Secreted and trans-membrane proteins are translocated into the ER and are properly folded and modified through a sophisticated ER quality control (ER QC) system to guarantee their functionality before being transported to their final destination (Liu and Howell, 2010). Under abiotic or biotic stress, unfolded or misfolded proteins often accumulate in the ER lumen, which results in the ER stress. To relieve ER stress and restore ER homeostasis, ER membrane-localized stress sensors such as the transcription factor bZIP28 subsequently activate the unfolded protein response (UPR) (Howell, 2013). The UPR includes the induction of ER chaperones and foldases, such as heat shock proteins (HSPs), protein disulfide isomerases (PDIs) and peptidyl prolyl *cis-trans* isomerases (PPIases) (Braakman and Hebert, 2013), which enhance protein folding in ER. In addition, the efficiency of protein translation is attenuated, global gene expression is inhibited, the capacity of protein secretion is potentiated and ER-associated protein degradation is induced in order to reinstall ER homeostasis, hence, functionality (Liu and Howell, 2010). In plants, there are at least two UPR pathways, which are mediated by IRE1-bZIP60 and bZIP28, respectively (Kørner et al., 2015). Increasing evidence suggests that adapting ER folding capacities and UPR regulation plays an important role in plant immunity. For example, the pattern-recognition receptor EFR requires the ER QC complex SDF2-ERdj3B-BiP for its proper processing (Nekrasov et al., 2009) and the secretion of pathogenesis-related proteins by *Arabidopsis* requires HSP AtBiP2

(Wang et al., 2005). Furthermore, the IRE1-bZIP60 branch of UPR is crucial for installing systemic acquired resistance (SAR) against bacterial pathogens and abiotic stress tolerance (Moreno et al., 2012). Interestingly, in rice the underlying SAR-mediating priming effect depends on *WRKY33*, a gene that is well-known to be involved in SA defense in *Arabidopsis* (Wakasa et al., 2014). In addition to supporting the production of plant immunity components ER stress can trigger, cell death can be part of an effective immune response but can be also deployed by some microbes to establish colonization (Qiang et al., 2012; Jing et al., 2016). Taken together, the ER has a significant effect on the outcome of plant-pathogen interactions. However, the molecular mechanisms of how ER-associated or regulated processes participate in plant immunity during the plant-pathogen interactions are not well understood.

Plant pathogenic oomycetes, such as *Phytophthora infestans*, *P. sojae* and *P. capsici*, cause many destructive crop diseases (Kamoun et al., 2015). They secrete a large number of effectors to facilitate plant infection. The first oomycete avirulence effector gene *Avr1b* was obtained by map-based cloning (Shan et al., 2004). Based on the sequences of cloned avirulence effectors, a conserved Arg-x-Leu-Arg (RXLR) motif in their N-terminal was found (Rehmany et al., 2005), which plays an important role in enabling effectors being delivered into host plant cells (Whisson et al., 2007; Dou et al., 2008; Kale et al., 2010; Wawra et al., 2017). Profiting from genome sequencing, hundreds of putative RXLR effector genes were predicted in each sequenced *Phytophthora* genomes (Tyler et al., 2006; Haas et al., 2009; Lamour et al., 2012). Their functions and underlying mechanisms have become a central focus of plant resistance and immunity research. Oomycete RXLR effectors have been shown to both directly hijack plant resistance pathways (McLellan et al., 2013; King et al., 2014; Du et al., 2015) and utilize plant susceptibility factors (Boevink et al., 2016; Wang et al., 2015; Yang et al., 2016). Interestingly, several RXLR effectors were found to interfere general host celluar processes, including ER stress-mediated cell death (Jing et al., 2016), autophagosome formation (Dagdas et al., 2016) and RNA silencing (Qiao et al., 2013; Qiao et al., 2015), to indirectly modulate plant immunity.

RXLR effectors are known to be highly diverse and effector sequences rarely overlap with each other across the genus (Jiang et al., 2008). However, the Avr3a effector family

105 represents an exception with various homologs in at least three different *Phytophthora* species,
106 i.e. *P. infestans*, *P. sojae* and *P. capsici* (Bos, 2007), implying the family has an important
107 role in *Phytophthora* pathogenicity. *P. sojae* and *P. infestans* have relatively narrow host
108 ranges and contain only a few copies of *Avr3a*-like effectors. In contrast, *P. capsici* infects a
109 broad range of hosts including 45 species of cultivated plants (Hausbeck and Lamour, 2004)
110 and its *Avr3a* gene family contains at least 13 homologs (*PcAvr3a1* to *PcAvr3a13*) (Bos, 2007.
111 It was reported that *P. infestans* effector PiAvr3a suppresses INF1-triggered cell death by
112 stabilizing CMPG1 (Bos et al., 2010) and inhibits PTI by associating with DRP2
113 (Chaparro-Garcia et al., 2015). PsAvr1b, an Avr3a homolog from *P. sojae*, suppresses
114 BAX-triggered cell death (Dou et al., 2008). However, all the 13 Avr3a homologs from *P.*
115 *capsici* were found neither to be recognized by potato resistance protein R3a nor suppress
116 INF1-triggered cell death (Bos, 2007), implying that they have more specialized roles in *P.*
117 *capsici* pathogenicity (Julio et al. 2014). To date, our understanding of the pathogenicity of *P.*
118 *capsici* and the role of its effectors, including these PcAvr3a homologs, remains elusive.

119 We previously reported that *P. capsici* is a pathogen of *Arabidopsis thaliana*, making it a
120 model oomycete pathosystem (Wang et al., 2013). In this project, we showed that *P. capsici*
121 employs the effector PcAvr3a12 as an efficient suppressor of various basic immune responses
122 to successful colonize *A. thaliana*. Our analyses revealed that the ER-localized FKBP15-2
123 protein, an PPIase, is a direct target of the effector and show the function of FKBP15-2 in the
124 regulation of ER stress processes as well as its regulatory function in plant immunity and how
125 this activity is modified by PcAvr3a12.

126 **RESULTS**

127 **Overexpression of *PcAvr3a12* Enhances Plant Susceptibility to *P. capsici* in *Arabidopsis***

128 Consistent with a previous study (Bos, 2007), our experiments showed that PcAvr3a12
129 could neither recognized by resistance protein R3a nor suppress INF1-triggered cell death
130 (Supplemental Figure 1) as reported for the well-studied *P. infestans* effector PiAvr3a, the
131 closest homolog to PcAvr3a12 in *P. capsici*. Using *A. thaliana* as a model host of *P. capsici*
132 (Wang et al., 2013), we infected the susceptible ecotype Col-0 with *PcAvr3a12*-expressing *P.*

*capsici* strain LT263. Real-time RT-PCR assays showed that *PcAvr3a12* was up-regulated during early infection, with a maximal expression level at 6 hours post inoculation (hpi) (Figure 1A). To examine the role of *PcAvr3a12* in *P. capsici* pathogenicity, *A. thaliana* Col-0 transgenic lines expressing *FLAG-PcAvr3a12* were generated and characterized (Figure 1D). Leaves of *FLAG-PcAvr3a12*-expressing lines showed larger water-soaked lesions than the *FLAG-GFP*-expressing control line, when inoculated with *P. capsici* zoospore suspensions (Figure 1B). RT-PCR analyses were performed (Llorente et al., 2010; Pan et al., 2016) to determine the *P. capsici* biomass in the same infected leaf area. The results consistently showed that *P. capsici* biomass were more abundant on *FLAG-PcAvr3a12*-expressing lines than on the *FLAG-GFP*-expressing control lines (Figure 1C). These data indicate that PcAvr3a12 could enhance the susceptibility of *A. thaliana* plants to *P. capsici* infection when overproduced in plant cells, and thus might function as a virulence factor.

**PcAvr3a12 Physically Interacts with a Host Protein, FKBP15-2**

To investigate how *PcAvr3a12* attenuates *A. thaliana* resistance against *P. capsici*, a yeast-two-hybrid (Y2H) library created from *P. parasitica*-infected *A. thaliana* cDNA was screened using *PcAvr3a12* for interacting proteins. This led to the identification of AtFKBP15-2 as a potential target of the PcAvr3a12. AtFKBP15-2 contains an N-terminal secretion signal, a FKBP domain and a C-terminal ER retention signal (Figure 2B) (He et al., 2004). Additional Y2H assays were used to validate the interaction between PcAvr3a12 and AtFKBP15-2. Therefore, PiAvr3a$^{KI}$, PcAvr3a14 (a PiAvr3a homolog cloned from *P. capsici* LT263; Supplemental Figure 2A), AtFKBP15-1 (the closest homolog of AtFKBP15-2 in *A. thaliana*; Figure 2B and Supplemental Figure 2B), PcFKBP35 (the blast best hit of AtFKBP15-2 in *P. capsici*; Supplemental Figure 2B) and respective empty vectors were used as controls in these Y2H assays. Yeast strain AH109 co-expressing *AtFKBP15-2* (the secretion signal peptide and ER retention signal of FKBP15-2 were truncated) and *PcAvr3a12* grew on selective medium and yielded β-galactosidase activity while all controls did not (Figure 2A), confirming the specific interaction between FKBP15-2 and PcAvr3a12 in yeast. Additionally, exchanges of *AtFKBP15-2* and *PcAvr3a12* between the prey plasmid (AD) and bait plasmid (BD) further confirmed this interaction even under conditions with higher selection pressure

(Figure 2C).

To further validate if the interaction can occur *in planta*, co-immunoprecipitation (Co-IP) assays were carried out. Therefore, p*35S::7*myc-PcAvr3a12* was constitutively co-expressed either with p*35S::SP-GFP-FKBP15-2-NDEL* (the GFP was fused with FKBP15-2 following its signal peptide), p*35S::*FLAG-GFP or the empty vector in *N. benthamiana* leaves through agroinfiltration. Total proteins were extracted from infiltrated leaves and were immunoprecipitated with GFP-Trap agarose beads. Immunoblotting experiments showed that, although 7*myc-PcAvr3a12 was equally expressed in all leaves, it was co-immunoprecipitated in *SP-GFP-FKBP15-2-NDEL*-expressing samples, but not in the FLAG-GFP or empty vector samples (Figure 2D and Supplemental Figure 3A). In similar experiments, FLAG-IP assays also showed that SP-directed GFP-FKBP15-2-NDEL was enriched with FLAG-PcAvr3a12, but not with FLAG-PiAvr3a$^{KI}$, although all proteins were detected in the input fractions (Supplemental Figure 3B-C). These results indicate that PcAvr3a12 associates with FKBP15-2 *in planta*.

**Expression of *FKBP15-2* is Up-regulated at the Early Stage of *Phytophthora* Infection**

To characterize the expression pattern of *FKBP15-2* during *P. capsici* infection, we measured its relative transcription levels at 0, 3, 6, 12, 24, 36, 48 and 60 hpi by RT-PCR. As observed for *PcAvr3a12* expression maxima (Figure 1A), *FKBP15-2* was up-regulated in Col-0 during early stage of *P. capsici* LT263 infection, reaching the highest expression level at 6 hpi (Figure 3A). Consistent with this, *FKBP15-2* transcripts were also up-regulated at early stages in *A. thaliana* (Col-0) roots inoculated with *P. parasitica* Pp016 zoospores (Figure 3B).

To further characterize the expression profile of *FKBP15-2*, a 1097-bp promoter fragment of *FKBP15-2* (-1097 to -1 bp) was cloned from genomic DNA to drive the expression of the *GUS* gene. This promoter was predicted using the online bioinformatics tool (http://arabidopsis.med.ohio-state.edu/AtcisDB). Stable transgenic *A. thaliana* (Col-0) lines carrying the reporter construct p*FKBP15-2::GUS* were generated and histochemical staining of the lines showed that GUS was activated by p*FKBP15-2* in the majority of organs, although to various degrees during all growth stages (Supplemental Figure 4).

## FKBP15-2 is Required for Plant Resistance to *Phytophthora*

To investigate the function of *FKBP15-2* in *Phytophthora* infection, we analyzed T-DNA mutant line *fkbp15-2* (Col-0 background) carrying a T-DNA insertion in the second intron region (Supplemental Figure 5A-B). The mutant showed similar growth phenotypes compared with Col-0 (Supplemental Figure 5C-D) despite a 98% reduction of *FKBP15-2* transcript (Figure 3C). Detached leaves of Col-0 and *fkbp15-2* plants were drop inoculated with *P. capsici* zoospores. The infection lesions on mutant *fkbp15-2* were larger than that on Col-0 (Figure 3D) and we observed more pathogen colonization (Figure 3E). Similarly, *fkbp15-2* leaves showed larger lesions (Figure 3F) and more pathogen biomass (Figure 3G) when infected with *P. parasitica* Pp016, suggesting that *FKBP15-2* is required for plant resistance against both *Phytophthora* spp. In support of this conclusion, analyses of *FKBP15-2* -overexpressing and -silenced *A. thaliana* transformants (Supplemental Figure 5E) showed significant changes in *P. capsici* colonization (Figure 3H). Considering that *P. parasitica* and *P. capsici* are two common soil-borne pathogens, with the former being less aggressive on Col-0, the roots of 2-week-old *fkbp15-2* and Col-0 seedlings were dip-inoculated with *P. parasitica* zoospores. Consistently, the pathogen biomass in *fkbp15-2* roots was higher than in Col-0 (Figure 3I). Furthermore, the expression of marker genes for the salicylic acid (SA) and jasmonic acid (JA) pathways, *PR1* and *PDF1.2*, respectively, (Uknes et al., 1993; Yun et al., 2003) that was reported to be induced by *Phytophthora* infection (Attard et al., 2010; Wang et al., 2013), was reduced at least by 60% as compared with that in Col-0 at 6 hpi (Supplemental Figure 6). Taken together, these results show that *FKBP15-2* is required for plant resistance to *Phytophthora* infection in *A. thaliana*.

## PcAvr3a12 Partially Associates with FKBP15-2 on the ER *in planta*

To investigate the subcellular localization of FKBP15-2 and its association with PcAvr3a12, mCherry or GFP fusions with each protein were used. p*35S::GFP/mCherry-PcAvr3a12* (PcAvr3a12 signal peptide was removed) and p*35S::SP-GFP/mCherry-FKBP15-2-NDEL* were constructed. All these GFP/mCherry fusions

were successfully expressed *in planta* as demonstrated by immunoblots (Supplemental Figure 7A-C). Consistent with previous prediction (He et al., 2004), SP-directed GFP-FKBP15-2-NDEL completely overlapped with the mCherry-labelled ER marker in the peri-nuclear ER and the ER network (Figure 4A), when they were co-expressed in *N. benthamiana* leaves. Moreover, GFP fluorescence of stable *SP-GFP-FKBP15-2-NDEL* -expressing *A. thaliana* leaves co-localized with ER-like networks and around the nucleus (Supplemental Figure 8A) without protein cleavage (Supplemental Figure 8B). We also found that GFP-SP-FKBP15-2-NDEL (GFP was tagged at the N terminus upstream of the signal peptide) was localized in the nucleus and cytoplasm (Supplemental Figure 9A-B), suggesting the N-terminal signal peptide was required for ER localization of FKBP15-2.

When GFP-PcAvr3a12 (lacking SP) was co-expressed with SP-directed mCherry-FKBP15-2-NDEL in *N. benthamiana* leaves, the two proteins could partially overlap at the peri-nuclear ER and the ER network, although GFP-PcAvr3a12 was also detectable in the cell nucleus and cytoplasm (Figure 4B). In addition, the plasma membrane and nucleus-localized GFP-PiAvrblb2 (Bozkurt et al., 2011) did not overlap with the SP-directed mCherry-FKBP15-2-NDEL (Supplemental Figure 9C). Furthermore, bimolecular fluorescence complementation (BiFC) assays, using N-terminal (VN) and C-terminal (VC) fragments of Venus fluorescent protein, were used to confirm whether PcAvr3a12 associates with FKBP15-2 in live plant cells. FKBP15-1 and PiAvr3a$^{KI}$ served as two independent controls in the BiFC assays. All of these fusion proteins were successfully expressed in *N. benthamiana* leaves without cleavage (Supplemental Figure 7D). Only the infiltrated leaves expressing SP-directed VN-FKBP15-2-NDEL and VC-PcAvr3a12 (lacking SP) showed obvious fluorescence in the ER-like structures (Figure 4C and 4F) in contrast to all control constructs (Figure 4D-E). We observed significantly more fluorescing cells in leaves co-infiltrated with *SP-VN-FKBP15-2-NDEL* and *VC-PcAvr3a12* as compared to the controls (Figure 4G). Taken together, these results suggest that PcAvr3a12 can at least partially associate with FKBP15-2 in the ER in live plant cells.

**PcAvr3a12 and FKBP15-2 Co-localize Around *Phytophthora* Haustoria During Infection**

To further examine subcellular localizations of FKBP15-2 and PcAvr3a12 during

*Phytophthora* infection, *N. benthamiana* leaves expressing GFP or mCherry fusions were inoculated with *Phytophthora* zoospores. Confocal microscopy showed that SP-directed mCherry-FKBP15-2-NDEL and mCherry-PcAvr3a12 proteins accumulated around the haustoria of GFP-labeled *P. parasitica* (Figure 5A, 5C and Supplemental Figure 10). Moreover, the ER was found to concentrate around haustoria during *Phytophthora* infection (Figure 5B). Consistent with this finding, infection with *P. capsici* consistently showed that GFP-PcAvr3a12 and SP-directed mCherry-FKBP15-2-NDEL were co-localized around haustoria-like structures (Figure 5D). Using PiAvrblb2, as a reported extrahaustorial membrane (EHM) marker during *Phytophthora* infection (Bozkurt et al., 2015), we further detected GFP-PcAvr3a12 co-localization with mCherry-PiAvrblb2 around haustoria-like structures (Figure 5E).

**The PPIase Activity of FKBP15-2 is Essential for Its Immune Function**

It was previously reported that the FKBP15-2 ortholog in *Vicia faba* possesses PPIase activity (Luan et al., 1996) and we therefore used conventionally protease-coupled PPIase assay to detect if FKBP15-2 has PPIase activity. The 93th residue (aspartic acid) in FKBP15-2 was predicted as an essential site for PPIase activity according to previous analyses (Lucke and Weiwad, 2011; Supplemental Figure 11A). Therefore, the maltose-binding protein (MBP) fusions, MBP-FKBP15-2, MBP-FKBP15-2$^{D93A}$ and MBP-GFP, were expressed in *E. coli*, purified by binding to amylose resin columns, and confirmed by both SDS-PAGE and immunoblots (Supplemental Figure 11B). The purified proteins were incubated with N-succinyl-ala-ala-pro-pNa, which can be cleaved by α-chymotrypsin to yield colored 4-nitroaniline, only when α-chymotrypsin has been converted to the trans-conformation by a PPIase. 4-nitroaniline production was faster with MBP-FKBP15-2 than with MBP-GFP or the spontaneous reactions (Figure 6A), indicating that FKBP15-2 possesses PPIase activity. Furthermore, 4-nitroaniline production with MBP-FKBP15-2$^{D93A}$ was slower than with MBP-FKBP15-2 (Figure 6A), consistent with loss of PPIase activity by FKBP15-2$^{D93A}$.

To confirm if the PPIase activity of FKBP15-2 is required for its contribution to immunity, *fkbp* mutant *A. thaliana* lines were complemented by transformation with p*FKBP15-2::FKBP15-2* or with p*FKBP15-2::FKBP15-2*$^{D93A}$. Two independent

complementation lines (CM), containing p*FKBP15-2::FKBP15-2*, and two independent mutant complementation lines ($CM^{D93A}$), containing p*FKBP15-2::FKBP15-2*$^{D93A}$, were confirmed by quantitative RT-PCR (Supplemental Figure 5F) and were chosen for infection assays with *P. capsici* zoospores. The water-soaked lesions on leaves of CM lines and Col-0 were smaller than on $CM^{D93A}$ lines (Figure 6C) with less pathogen colonization at 60 hpi (Figure 6D) while the water-soaked lesions on leaves of CM lines and Col-0 were similar (Figure 6C) with no significant difference in pathogen colonization (Figure 6D). These results indicate that the PPIase activity of FKBP15-2 is required for its contribution to immunity against *Phytophthora*.

**PcAvr3a12 Directly Suppresses the PPIase Activity of FKBP15-2**

Based on our result that the PPIase activity of FKBP15-2 is essential for its contribution to immunity, we investigated if the PPIase activity is affected by PcAvr3a12 in a protease-coupled *in vitro* assay. All purified recombinant proteins in these PPIase activity assays were confirmed by SDS-PAGE and immunoblots (Supplemental Figure 11C). The PPIase activity of MBP-FKBP15-2 incubated with MBP-PcAvr3a12, MBP-PcAvr3a14 and rapamycin (a chemical inhibitor of PPIase), respectively, was detected as described before (Harding *et al*., 1989). Here, MBP-PcAvr3a14 and rapamycin were used as controls. In the presence of PcAvr3a12 or rapamycin, the PPIase activity of MBP-FKBP15-2 was lower than in the presence of PcAvr3a14 (Figure 6B), suggesting that the PPIase activity of FKBP15-2 was attenuated by binding to PcAvr3a12. We also examined whether PcAvr3a12 affects the *in vivo* stability of FKBP15-2. The *FKBP15-2-GFP* fusion was co-expressed with *FLAG-PcAvr3a* or free *mCherry* in *N. benthamiana* leaves by agroinfiltration. The results showed that the accumulation of SP- directed GFP-FKBP15-2-NDEL was not significantly different between the *FLAG-PcAvr3a12* co-expressing tissue and *mCherry* co-expressing tissue (Figure 6E).

***FKBP15-2* is Involved in General UPR Induction and ER Stress-Mediated Plant Immunity**

The protein folding capacity of the ER have been demonstrated to be crucial for rapid

and effective basal immune responses (Kørner et al., 2015). Our findings that FKBP15-2 was identified to localize in the ER and shows PPIase activity, prompted us to question whether *FKBP15-2* regulates ER stress to mediate its contribution to immunity against *Phytophthora* spp. To test this, 5-day-old seedlings of Col-0 and the *fkbp15-2* mutant were treated with ER stress inducer/N-glycosylation inhibitor tunicamycin (TM) or dimethyl sulfoxide (DMSO) as control. At 7 days post treatment, the fresh weight of the seedlings was measured. The results showed around 50% reduction in fresh weight for the TM-treated Col-0 seedlings compared with that of the DMSO-treated seedlings. In contrast, in the *fkbp15-2* mutants, TM treatment resulted in only about 17% biomass reduction compared with control seedlings (Figure 7C), suggesting that *FKBP15-2* might contribute to sensing of TM-induced ER stress.

To further examine whether *FKBP15-2* contributes to ER stress sensing and subsequent UPR regulation, 12-day-old Col-0 and *fkbp15-2* seedlings o were spray treated with TM and the transcript levels of ER stress sensor genes, *bZIP60* and *bZIP28*, and UPR marker gene *BiP3* were monitored by real-time quantitative RT-PCR. The results showed that the levels of *bZIP60*, spliced *bZIP60* (ER stress-activated form of *bZIP60*) and *BiP3* were significantly elevated in Col-0 by TM. However, the elevation of *bZIP60*, spliced *bZIP60* and *BiP3* levels were significantly attenuated in the *fkbp15-2* mutants at 6 hours post TM treatment (Figure 7A). Although *bZIP28* was not clearly elevated by TM treatment, its transcript level was reduced in the *fkbp15-2* mutants as compared to Col-0 (Figure 7A). These results indicate that *FKBP15-2* contributes to general ER stress sensing and UPR regulation, although there was no obvious elevation of *FKBP15-2* transcripts in the TM-treated Col-0 (Supplemental Figure 12B).

To investigate if the contribution of *FKBP15-2* o immunity is related to its contribution to ER stress and UPR regulation, we examined the transcript levels of ER stress sensor genes *bZIP60*, *bZIP28* and *BiP3* during early biotrophic colonization by *P. capsici*. For this, leaves of 4-week-old Col-0 and *fkbp15-2* mutants were inoculated with *P. capsici* zoospores, harvested at 0, 3, 6 and 12 hpi for quantitative RT-PCR analyses. The results showed that the levels of *bZIP60* and *BiP3* in Col-0 were elevated at early infection stages of infection by *P. capsici*, while only slight elevation of *bZIP28*, if any, was observed. In contrast, the transcript

levels of *bZIP60*, *bZIP28* and *BiP3* in the *fkbp15-2* mutants upon infection by *P. capsici* were significantly attenuated during early infection (Figure 7B). In accordance with this, several immunity-related genes were obviously induced upon infection by *P. capsici* in the Col-0 plants, including *γVPE* (ER stress-mediated cell death gene), *WRKY33* (UPR-mediated SAR priming gene), *EFR* (ER-QC dependent pattern-recognition receptor) and *CYP81F2* (a *P. capsici* resistance gene encoding an ER localized indole glucosinolate biosynthesis enzyme gene; Wang et al., 2013) (Figure 7B). However, in the *fkbp15-2* mutant the elevations of *WRKY33*, *EFR* and *CYP81F2* were significantly reduced during early infection compared with Col-0, especially at 6 and 12 hpi) (Figure 7B). Similarly, when 12-day-old-seedlings were inoculated with *P. parasitica*, the expression levels of ER stress sensors (*bZIP60* and *bZIP28*) and ER stress-mediated immunity genes (*γVPE*, *WRKY33* and *EFR*) were lower during early infection in *fkbp15-2* mutants than Col-0 (Supplemental Figure 12A). Taken together, these results imply that *FKBP15-2* contributes to ER stress-mediated plant immunity.

## DISCUSSION

Plant pathogens secrete effectors to interfere with plant immune response to promote colonization (Jones and Dangl, 2006). PiAvr3a is a well-known RXLR effector from *P. infestans* that plays an essential role in pathogenesis (Bos et al., 2010; Gilroy et al., 2011; Chaparro-Garcia et al., 2015). Avr3a-family effectors are among the few RXLR effectors that are relatively well conserved across diverse *Phytophthora* species and are highly expanded in *P. capsici* (Bos, 2007), suggesting their importance in pathogenesis and that they may have evolved specialized roles in *P. capsici* (Vega-Arreguin et al. 2014). Our results showed that *PcAvr3a12* is highly upregulated during early infection and expression *in planta* renders the host plant *A. thaliana* more susceptible to *P. capsici* (Figure 1), supporting its role as a virulence effector, consistent with the virulence role of Avr3a family effectors PiAvr3a (Bos et al., 2010) and PsAvr1b (Dou et al., 2008). In contrast to PiAvr3a and PsAvr1b, respectively, PcAvr3a12 cannot be recognized by R3a, nor suppress INF1-triggered cell death (Supplemental Figure 1), suggesting it has evolved a more specialized role in *P. capsici*. Accordingly, PcAvr3a12 was found to have a distinct host target, AtFKBP15-2, that we found

362 through Y2H screening and confirmation by Y2H, Co-IP and BiFC assays (Figure 2 and
363 Figure 4C-G).

364 In plants, there are three PPIase families, including cyclophilins (CYPs), FK506- and
365 rapamycin-binding proteins (FKPBs), and parvulins (He et al., 2004). Two plant CYPs,
366 ROC1 (Coaker et al., 2005) and GmCYP1 (Kong et al., 2015), were identified to be required
367 for activation of specific effectors through allosteric transition of peptidyl-prolyl bonds in the
368 effectors. In the case of PcAvr3a12, however, there is no proline in the mature protein,
369 consistent with different mechanism of interaction between FKBP15-2 and PcAvr3a12.

370 FKBP family members are involved in diverse aspects of cellular physiology including
371 hormone signaling, protein trafficking, transcription, plant growth and stress response (Harrar
372 et al., 2001; Romano et al., 2005). However, the specific roles of many FKBPs in plants
373 remain unclear (Vasudevan et al., 2015). *AtFKBP65*, a homolog of *AtFKBP15-2*, was recently
374 reported to be responsive to *Pseudomonas syringae* infection and to be required for callose
375 accumulation (Pogorelko et al., 2014). Our results showed that *FKBP15-2* is responsive to
376 *Phytophthora* infection (Figure 3A-B) and positively contributes to plant resistance (Figure
377 3C-I). We have also detected peptidyl-prolyl *cis-trans* isomerase activity for FKBP15-2 in
378 protease-coupled assays (Figure 6A), as reported for its ortholog in *V. faba* (Luan et al., 1996).
379 In accordance with previous work (Lucke and Weiwad, 2011), mutating an essential residue
380 (FKBP15-2$^{D93A}$) weakened its PPIase activity (Figure 6A). Further pathogenicity assays on
381 *FKBP15-2*$^{D93A}$ and *FKBP15-2* complementation lines showed that the PPIase activity of
382 FKBP15-2 is important for its immunity-associated function against *Phytophthora* infection
383 (Figure 6C-D). Together with our result that PcAvr3a12 directly suppresses PPIase activity of
384 FKBP15-2 *in vitro* (Figure 6B), we conclude that *PcAvr3a12* attenuates plant immunity by
385 suppressing PPIase activity of FKBP15-2.

386 *Trans-cis* isomerization activity mediated by PPIases are crucial for protein folding,
387 since the majority of proteins have prolyl residues (Braakman and Hebert, 2013). It is
388 well-documented that proline isomerization is a slow process and rate-limiting for protein
389 folding (Brandts et al., 1977; Lang et al., 1987). In addition, ER localized molecular
390 chaperones and foldases generally form complexes to modulate protein modification and

folding, which is an important part of the UPR (Jansen et al., 2012). The ER-localized BiP chaperones regulate UPR signaling after dissociation from the ER stress sensor IRE1 (Bertolotti et al. 2000). Both *VfFKBP15* from *V. faba* and *ScFKBP2* from *Saccharomyces cerevisiae* are orthologs of *AtFKBP15-2* and *AtFKBP15-1*. The *VfFKBP15* gene was highly up-regulated under heat shock stress (Luan et al., 1996) and the *ScFKBP2* was highly up-regulated under treatment with ER stress inducer tunicamycin (TM) (Partaledis & Berlin, 1993), implying that they have a key role in protein folding. Different from these two orthologs, there was no obvious induction of *AtFKBP15-2* in Col-0 under TM treatment (Supplemental Figure 12B), implying a different role of *AtFKBP15-2* in *A. thaliana* or, alternatively, a post-transcriptional regulation of *AtFKBP15-2*. In our study, the *fkbp15-2* mutants exhibited an insensitivity to TM treatment (Figure 7C). Furthermore, the TM-triggered induction of ER stress sensor genes (*bZIP60*, spliced *bZIP60*, and *bZIP28*) and a UPR marker gene (*BiP3*) were significantly reduced in the *fkbp15-2* mutants as compared to Col-0 (Figure 7A). These results suggest that *FKBP15-2* is (directly or indirectly) involved in the transcription of ER stress sensors, *bZIP60* and *bZIP28*, and subsequent UPR pathways. FKBPs do not only help protein folding but also modulate signal transduction pathways by changing the conformation of interacting proteins (Harrar et al., 2001). Thus, further identification of FKBP15-2-interacting proteins will facilitate the elucidation of the mechanisms by which FKBP15-2 affects transcription of ER stress sensors and regulation of the UPR pathways.

There is clear evidence that ER stress response contributes to plant immunity in several ways, including the processing of pattern recognition receptors, the regulation of the anti-microbial protein secretion, and priming of SAR and ER stress-mediated cell death (Wang et al., 2005; Li et al., 2009; Moreno et al., 2012; Qiang et al., 2012; Kørner et al., 2015). It was recently shown that GmBiPs were targeted by *P. sojae* RXLR effector PsAvh262, resulting in the attenuation of ER stress-mediated cell death (Jing et al., 2016), which suggests that one way that microbes achieve compatibility is through manipulation of plant ER stress by effectors. In addition to an altered expression of ER stress sensing and UPR marker genes (Figure 7B), mutants lacking the PcAvr3a12 target FKBP15-2 displayed an

attenuated induction of two known ER stress-mediated plant immunity maker genes, *EFR* and *WRKY33*, during the early infection of *Phytophthora* (Figure 7B; Supplemental Figure 12A). Further, ER stress-mediated cell death maker gene *γVPE* was attenuated in *fkbp15-2* mutants during the early infection of *P. parasitica* (Supplemental Figure 12A) as was the expression of secreted immunity-related protein genes (*PR1* and *PDF1.2*) (Supplemental Figure 6) and ER -localized *P. capsici* resistance gene *CYP81F2* (Wang et al., 2013) (Figure 7B) in *fkbp15-2* mutants at the early *P. capsici* infection. These results suggest that *FKBP15-2* positively contributes to plant resistance most likely by participating in ER stress response pathways. Future studies on silencing or knockout of *PcAvr3a12* in *P. capsici* may further confirm whether this effector directly disturbs the host UPR.

Since the signal peptide of FKBP15-2 is essential for its ER localization (Figure 4A and Supplemental Figure 9), it is likely that the translation of FKBP15-2 is completed at ER and thus that mostly FKBP15-2 reaches the ER by the co-translational pathway, which may explain why PcAvr3a12 is not significantly enriched by FKBP15-2 to ER during co-expression (Figure 4B). Our subcellular localization (Figure 4B) and BiFC (Figure 4C-G) assays indicate that even lacking its signal peptide, some of the PcAvr3a12 expressed in plant cells overlapped with FKBP15-2 in the ER in healthy plant cells. The way PcAvr3a12 enters the ER structures during high level over-expression in plant cells remains unclear. It is possible that a fraction of FKBP15-2 is post-translationally targeted to the ER, and that that fraction is sufficient to bind to PcAvr3a12 and carry it into the ER. During natural infection, effectors are thought to enter plant cells via some formation of endocytosis, which would target them to the lumen of the endomembrane system, from where they could undergo retrograde trafficking to the ER. Currently, the translocation route and subcellular localization of *Phytophthora* effectors are difficult to be directly observed during infection (Wang et al., 2017). However, our localization assays of FKBP15-2 and PcAvr3a12 during infection showed that both of them accumulated and co-localized around haustoria, further supporting their interaction (Figure 5 and Supplemental Figure 10). Taken together, we propose that during early infection *P. capsici* secretes the RXLR effector PcAvr3a12 to target the ER-localized PPIase FKBP15-2 around haustoria to suppress plant immunity (Figure 8).

Targeting of FKBP15-2 seems to be especially relevant for *P. capsici* infection due to its participation in maintaining ER homeostasis.

## MATERIAL AND METHODS

### Plasmid Constructs

To create yeast-two-hybrid constructs, the coding regions of *AtFKBP15-2*, *AtFKBP15-1*, *PcAvr3a12*, *PcAvr3a14* and *PcFKBP35* without secreted signal peptide and ER retention peptide, were cloned from Col-0 or LT263 cDNA and inserted into pGADT7 and pGBKT7 with *Eco*RI and *Bam*HI sites. To create bimolecular fluorescence complementation (BiFC) constructs, the fusion fragments of *SP-VN-FKBP15-2-NDEL* and *SP-VN-FKBP15-1-KDEL* were obtained through overlapping PCR and inserted into pDEST-$^{GW}$VYNE (Gehl et al. 2009) with *Spe*I and *Sac*I. The coding sequence of *PcAvr3a12* and *PiAvr3a*$^{KI}$ without signal peptide were inserted into pDEST-VYCE$^{GW}$ (Gehl et al. 2009) with *Spe*I and *Xho*I. To prepare overexpression constructs, the full-length of *FKBP15-2* was cloned from Col-0 cDNA and inserted into pKannibal (Wesley et al., 2001) with *Eco*RI and *Bam*HI sites, then inserted into the binary vector pART27 (Gleave, 1992) at the *Not*I site. To create eGFP/mCherry/7*myc-fusion plasmids, we firstly cloned eGFP/mCherry/7*myc fragment into pKannibal with *Xho*I and *Eco*RI sites and inserted into pART27 at *Not*I site. Mature PcAvr3a12 and full-length FKBP15-2 coding sequence was inserted into previous modified pART27 with *Eco*RI and *Xba*I sites to create *GFP/mCHerry/7*myc-PcAvr3a12* and *GFP-SP-FKBP15-2-NDEL*. For other plant expression constructs, including *SP-GFP/mCherry-FKBP15-2-NDEL*, *FLAG-PiAvr3a*$^{KI}$ and *FLAG-PcAvr3a12* fusion fragments were obtained from restriction enzyme digestion or overlapping PCR and replaced previous plant expression vector with *Xho*I and *Xba*I sites. To generate the RNA silencing vector, a specific 250-bp fragment (61-310 bp) was chosen with no wrong-target effects and inserted into pKannibal vector between the *Xho*I-*Eco*RI sites with sense orientation and the *Cla*I-*Xba*I sites with antisense orientation to compose a hairpin. Finally, hairpin was transferred into pART27 from this assembled pKannibal through *Not*I site. To construct the p*FKBP15-2::GUS* reporter vector, a 1097-bp promoter fragment of *FKBP15-2* was amplified from Col-0 genomic DNA and inserted into the binary vector pMDC162 (Curtis and

Grossniklaus, 2003) with *Kpn*I and *ASC*I sites. We constructed other p*FKBP15-2* promoter derived vectors by replacing GUS sequence with *ASC*I and *Sac*I sites on this assembled GUS vector, including p*FKBP15-2::FKBP15-2* and p*FKBP15-2::FKBP15-2*$^{D93A}$. The plant expression vector of ER-maker is obtained from ABRC (stock number CD3-959) (Nelson et al., 2007). To create prokaryotic expression vectors, a modified pET21a with a MBP tag fused at its N terminus was used. The coding fragments of *FKBP15-2*, *FKBP15-2*$^{D93A}$, *PcAvr3a12* and *PcAvr3a14* without secretion and ER-retention signal peptide encoding sequences were inserted into previous modified pET21a-MBP with *Eco*RI and *Xho*I sites. All these vectors were verified by sequencing. All the previous used primers are listed in Supplemental Table 1.

**Plant Materials and Growth Conditions**

The *FKBP15-2* T-DNA insertion line (SALK_113542) was obtained from the ABRC. Homozygosity of T-DNA insertion mutants were confirmed by PCR using primers FP (GATTATGGCGAGCAAGATGAG), RP (ATCCCTCATCATCTTCATCCC) and BLa1 (TGGTTCACGTAGTGGGCCATCG). All transgenic *A. thaliana* lines were generated by floral dip method (Zhang et al., 2006) and screened on half-strength Murashige and Skoog (1/2 MS) plates with corresponding antibiotics. Plant growing conditions for *A. thaliana* and *N. benthamiana* were as previously described (Pan et al., 2016).

**Yeast-Two-Hybrid Assay**

The yeast-two-hybrid library screening and yeast two-hybrid (Y2H) assays were performed using the Matchmaker Two-Hybrid System 3 protocol (Clontech). To screen the yeast-two-hybrid library, the pGBKT7 vector containing effector gene, acting as a bait, was transformed into yeast strain Y187. Positive yeast clones were mated with AH109 containing cDNA from *P. parasitica* infected *A. thaliana* tissue, and then the diploids were plated on SD/-Trp-Leu-His-Ade medium. We picked colonies from SD/-Trp-Leu-His-Ade medium to verify their sequence. For the Y2H assay, pGBKT7 and pGADT7 vectors, each containing selection gene, were co-transformed into the yeast strain AH109. Transformations were checked on SD/-Trp-Leu medium and interactions were confirmed by the growth on SD/-Trp-Leu-His medium adding with 2.5mM 3-amino-1, 2, 4-triazole (3AT), gain of

β-galactosidase activity (β-gal) or the growth on SD/-Trp-Leu-His-Ade medium.

**Agroinfiltration and Confocal Laser Scanning Microscopy**

*Agrobacterium tumefaciens* strain (GV3101) transformed with vector constructs was grown at 28°C for about 36 hours in LB medium with appropriate antibiotics. *Agrobacterium* were pelleted, resuspended in infiltration buffer (10 mM MES, 10 mM MgCl2 and 200 µM acetosyringone), adjusted to the required concentration ($OD_{600}$ approximate 0.1-0.3) and infiltrated into 4- to 6-week-old *N. benthamiana* leaves.

Confocal images were taken using an Olympus IX83 confocal microscopy (Japan) and infiltrated *N. benthamiana* leaves or stable transgenic *A. thaliana* leaves. GFP and Venus expression was detected after excitation at 488 nm wavelength laser and their emissions were collected between 500 nm to 540 nm. The fluorescence of mCherry was excited with 559 nm wavelength laser to detected specific emissions between 600 nm and 680 nm.

**Co-immunoprecipitation Assays**

Three days after agroinfiltration, *N. benthamiana* leaves were detached and ground with liquid nitrogen by mortar and pestle. Proteins were extracted with GTEN lysis buffer (10% glycerol, 25 mM Tris pH 7.5, 1 mM EDTA, 150 mM NaCl) supplemented with 2% w/v PVPP, 10 mM DTT, 1×protease inhibitor cocktail (Sigma) and 0.1% Tween 20 (Sigma) and precipitated by GFP-Trap agarose beads (Chromotek) or Anti-FLAG M2 affinity Gel (Sigma) as described (Win et al., 2011). Precipitates were washed at least five times by GTEN buffer supplemented with 0.1% Tween 20. Fusion proteins from crude extracts (input) and precipitated proteins were detected by immunoblots by protein-specific antibodies.

**Protein Immunoblot Assays**

Proteins were separated by sodium dodecyl sulphate-polyacrylamide gel electrophoresis (SDS–PAGE) and transferred from the gel to a PVDF membrane (Roche) in transfer buffer (25 mM Tris, 200 mM glycine and 20% methanol). The transferred membrane was blocked in TBST (pH 7.2, TBS with 0.05% Tween 20) containing 10% non-fat dry milk under gentle shaking. The blocked membrane was incubated with specific antibodies which was dissolved

in TBSTM (TBST with 5% non-fat dry milk) at a ratio of 1: 2000 and incubated at 4$^{o}$C with shaking at 50 rpm overnight, followed by three washes (10 min each) with TBST. Next, the membrane was incubated with a secondary antibody coupling with HRP which was also dissolved into TBSTM at a ratio of 1: 2000 at room temperature for 1.5 hours under shaking. There after the membrane was washed three times (10 min each) with TBST, one time with TBS, then incubated with ECL (#CW0049S, ComWin) before photographing using a molecular imager (ChemiDoc$^{TM}$ XRS+, Bio-Rad). The first antibodies used in our experiments include anti-FLAG (#AE005; ABclonal), anti-GFP (#AE012, ABclonal), anti-myc (#AE010, ABclonal), and anti-HA (#HT301-01, Transgen). The second antibodies include HRP Goat anti-Mouse IgG (H+L) antibody (#AS013, ABclonal) and HRP goat anti-rabbit IgG (H+L) antibody (#AS014, ABclonal).

**_P. parasitica_ and _P. capsici_ Culture Conditions and Inoculation Assays**

The culture and zoospore production of *P. parasitica* and *P. capsici* were conducted as previously reported (Wang et al., 2011; Wang et al., 2013). The culture medium for both *P. parasitica* and *P. capsici* was 5% (v/v) cleared carrot juice (CA) medium containing 0.002% (w/v) β-sitosterol and 0.01% (w/v) $CaCO_3$. The *P. capsici* strain used in this study was LT263. The *P. parasitica* strain used in this study was Pp016.

For *P. capsici* inoculation assays, detached *A. thaliana* leaves were inoculated on the abaxial leaf surface with a 10 μL droplet containing ~80 *P. capsici* zoospores μL$^{-1}$. Leaf discs (diameter 1 cm) from around the zoospore droplets were collected with a puncher from at least eight leaves at 60 hpi for one sample in each line. Genomic DNA was extracted by the CTAB method and the pathogen biomass was quantified by real-time PCR as previously reported (Llorente et al., 2010). The results represented the proportion between pathogen and plant genomic DNA and statistical significances were determined by one-way ANOVA followed by Tukey's multiple comparison test. The *P. parasitica* inoculation assays were performed similarly described as above except that each leaf was wounded by toothpicks and inoculated with a 10 μL droplet with 200 *P. parasitica* zoospores μL$^{-1}$ at wound sites. *P. parasitica* infected leaf discs were collected at 72 hpi. For *P. parasitica* root inoculation, roots of 14-day-old seedlings were dipped into a zoospore suspension (200 spores/μL) for 10 s and

transferred to petri dishes containing half-strength Murashige and Skoog (MS) medium without sugar. The root tissues of about 24 seedlings were pooled together for one sample. Pathogen biomass was quantitated by RT-PCR as described above. All primers used can be found in Supplemental Table S2. The data diagrams were drawn by OriginPro.

**Gene Expression Analyses**

Total RNAs were extracted by using TRIzol (Invitrogen) reagent. For quantitative real-time reverse transcription-PCR (RT-PCR), cDNA was synthesized from 800 ng of total RNA using PrimeScript$^{TM}$ RT reagent Kit (TaKaRa). Real-time PCR reactions were performed using 5 μL template from a 1:20 dilution by SYBR Premix Kit (Roche) according to manufacturers' instructions. The primers we used are listed in Supplemental Table 2. The Ct values of genes were quantified using an iQ7 Real-Time Cycler (Life Technologies, USA). Expression fold changes were calculated by the $2^{-\Delta\Delta Ct}$ method. Statistical significance was determined by one-way ANOVA followed by Tukey's multiple comparison test. The data diagrams were drawn by OriginPro.

**Recombinant Protein Expression and Purification**

Constructs for production of recombinant MBP-GFP, MBP-PcAvr3a12, MBP-PcAvr3a14, MBP-FKBP15-2 and MBP-FKBP15-2$^{D93A}$ proteins were introduced into *E. coli* strain BL21 (DE3). Cultures were incubated for 8 hours with 0.4 mM IPTG at 25-28$^{o}$C under shaking at 180 rpm after $OD_{600}$ of 0.5-0.6 at 37$^{o}$C. Cells were pelleted and resuspended with ice-cold lysis buffer (20 mM Hepes, 5 mM β-mercaptoethanol, 1 mM EDTA, 150 mM NaCl, pH 7.5) containing 1×cocktail (Sigma). The resuspended cells were sonicated and centrifuged at 20,000*g* for 30 minutes at 4$^{o}$C. Crude proteins were affinity purified by amylose affinity chromatography (NEB) and washed from the amylose resin column with wash buffer (20 mM Hepes, 5 mM β-mercaptoethanol, 1 mM EDTA, 150 mM NaCl). Fusion proteins were eluted with wash buffer containing 10 mM maltose and were concentrated by centrifugation through an ultrafiltration tube (Merck). After purification, the purity of proteins was determined by SDS-PAGE and immunoblotting.

**Rotamase (PPIase) Activity Assays**

The rotamase activity of the recombinant FKBP15-2 or FKBP15-2$^{D93A}$ proteins was determined through the chymotrypsin coupled assays (Harding *et al*., 1989). The purified recombinant proteins in assay buffer (40 mM HEPES, 0.015% Triton X-100, 150 mM NaCl, pH 7.9) were mixed with 37.5 μL of 5.6 nM succinyl-Ala-Leu-Pro-Phe-paranitroanilide (#S8511, Sigma), to generate a 2910 μL mixture. That mixture was transferred into a cuvette before being placed in a UV/VIS spectrophotometer at 8$^{o}$C. Each sample was pre-cooled at 8$^{o}$C before measurement. The reactions were initiated by adding 90 μL of 50 mg/mL chymotrypsin (#C3142, Sigma) and were monitored by measuring absorbance at 390 nm every second for 5 min. The rapamycin, an inhibitor of PPIases, was obtained from Sigma (#V900930).

**Accession numbers**

Sequence data from this article can be found in the Arabidopsis genome data library (http://www.arabidopsis.org/), genome bank data library (https://www.ncbi.nlm.nih.gov/) or *P. capsici* genome data library (https://genome.jgi.doe.gov/Phyca11/Phyca11.home.html). Accession numbers: At3g25220, AtFKBP15-1; At5g48580, AtFKBP15-2; PITG_14371, PiAvr3a$^{KI}$; jgi|Phyca11|114071, PcAvr3a12; jgi|Phyca11|113768, PcAvr3a14; jgi|Phyca11|510076, PcFKBP35.

**AUTHOR CONTRIBUTIONS:**

W.S. and G.F. conceived and designed the experiments. G.F., Y.Y., W.L., T.L., and Q.W. performed the experiments. T.L. screened the yeast-two-hybrid library. G.F., X.Q. and W.S. analyzed the data. G.F., Y.D., X.Q., and W.S. wrote the manuscript. All authors reviewed the manuscript.

**ACKNOWLEDGEMENTS:**

We thank Dr. Brett Tyler (Oregon State University, USA), Dr. Patrick Schäfer (University of Warwick, UK), and Dr. Mingbo Wang (CSIRO Agriculture, Canberra, Australia) for their insightful suggestions, Dr. Gary Loake (University of Edinburgh, UK) for advice on the PPIase activity assays, Xuguang Xi (Northwest A&F University, China) for providing

modified pET21a-MBP plasmid and assistance in protein purification, and Brett Tyler and Patrick Schäfer for manuscript editing. This work was supported by China Agriculture Research System (CARS-09), the National Natural Science Foundation of China (31125022 and 31561143007), and the Programme of Introducing Talents of Innovative Discipline to Universities (Project 111) from the State Administration of Foreign Experts Affairs (#B18042).

**REFERENCE:**

**Attard, A., Gourgues, M., Callemeyn-Torre, N., and Keller, H.** (2010). The immediate activation of defense responses in Arabidopsis roots is not sufficient to prevent *Phytophthora parasitica* infection. New Phytologist **187**: 449–460.

**Bertolotti, A., Zhang, Y., Hendershot, L.M., Harding, H.P., and Ron, D.** (2000). Dynamic interaction of BiP and ER stress transducers in the unfolded-protein response. Nature Cell Biology **2**: 326-332.

**Boevink, P.C., Wang, X., McLellan, H., He, Q., Naqvi, S., Armstrong, M.R., Zhang, W., Hein, I., Gilroy, E.M., Tian, Z., et al.** (2016). A *Phytophthora infestans* RXLR effector targets plant PP1c isoforms that promote late blight disease. Nature Communications **7**: 10311.

**Bos, J.I.B.** (2007). Function, structure and evolution of the RXLR effector AVR3a of *Phytophthora infestans*. PhD thesis. The Ohio State University, Columbus, OH, USA.

**Bos, J.I.B., Armstrong, M.R., Gilroy, E.M., Boevink, P.C., Hein, I., Taylor, R.M., Zhendong, T., Engelhardt, S., Vetukuri, R.R., Harrower, B., et al.** (2010). *Phytophthora infestans* effector AVR3a is essential for virulence and manipulates plant immunity by stabilizing host E3 ligase CMPG1. Proceedings of the National Academy of Sciences USA **107**: 9909-9914.

**Bozkurt, T.O., Belhaj, K., Dagdas, Y.F., Chaparro-Garcia, A., Wu, C.H., Cano, L.M., and Kamoun, S.** (2015). Rerouting of plant late endocytic trafficking toward a pathogen interface. Traffic **16**: 204-226.

**Bozkurt, T.O., Schornack, S., Win, J., Shindo, T., Ilyas, M., Oliva, R., Cano, L.M., Jones,**

**A.M.E., Huitema, E., Hoorn, R.A.L.V.D., et al.** (2011). *Phytophthora infestans* effector AVRblb2 prevents secretion of a plant immune protease at the haustorial interface. Proceedings of the National Academy of Sciences USA **108**: 20832-20837.

**Braakman I., and Hebert D.N.** (2013). Protein folding in the endoplasmic reticulum. Cold Spring Harbor Perspectives in Biology **5**: a013201

**Brandts, J.F., Brennan, M., and Lung-Nan, L.** (1977). Unfolding and refolding occur much faster for a proline-free proteins than for most proline-containing proteins. Proceedings of the National Academy of Sciences USA **74**: 4178-4181.

**Chaparro-Garcia, A., Schwizer, S., Sklenar, J., Yoshida, K., Petre, B., Bos, J.I.B., Schornack, S., Jones, A.M.E., Bozkurt, T.O., and Kamoun, S.** (2015). *Phytophthora infestans* RXLR-WY effector AVR3a associates with Dynamin-Related Protein 2 required for endocytosis of the plant pattern recognition receptor FLS2. PLoS ONE **10**: e0137071.

**Coaker, G., Falick, A., and Staskawicz, B.** (2005). Activation of a phytopathogenic bacterial effector protein by a eukaryotic cyclophilin. Science **308**: 548-550.

**Curtis, M.D., and Grossniklaus, U.** (2003). A gateway cloning vector set for high-throughput functional analysis of genes in planta. Plant Physiology **133**: 462-469.

**Dagdas, Y.F., Belhaj, K., Maqbool, A., Chaparro-Garcia, A., Pandey, P., Petre, B., Tabassum, N., Cruz-Mireles, N., Hughes, R., Sklenar, J., et al.** (2016). An effector of the Irish potato famine pathogen antagonizes a host autophagy cargo receptor. eLife **5**: e10856.

**Dodds P.N., and Rathjen J.P.** (2010). Plant immunity: towards an integrated view of plant–pathogen interactions. Nature Reviews Genetics **11**: 539-548.

**Dou, D., Kale, S.D., Wang, X., Chen, Y., Wang, Q., Wang, X., Jiang, R.H.Y., Arredondo, F.D., Anderson, R.G., Thakur, P.B., et al.** (2008). Conserved C-terminal motifs required for avirulence and suppression of cell death by *Phytophthora sojae* effector Avr1b. Plant Cell **20**: 1118-1133.

**Dou D., and Zhou J.M.** (2012). *Phytopathogen* effectors subverting host immunity: different foes, similar battleground. Cell Host and Microbe **12**: 484-495.

**Du, Y., Mpina, M.H., Birch, P.R.J., Bouwmeester, K., and Govers, F.** (2015). *Phytophthora infestans* RXLR effector AVR1 interacts with exocyst component Sec5 to manipulate plant immunity. Plant Physiology **169**: 1975-1990.

**Gehl, C., Waadt, R., Kudla, J., Mendel, R.R., and Hänsch, R.** (2009). New GATEWAY vectors for high throughput analyses of protein–protein interactions by bimolecular fluorescence complementation. Molecular Plant **2**: 1051-1058.

**Gilroy, E.M., Taylor, R.M., Hein, I., Boevink, P., Sadanandom, A., and Birch, P.R.J.** (2011). CMPG1-dependent cell death follows perception of diverse pathogen elicitors at the host plasma membrane and is suppressed by *Phytophthora infestans* RXLR effector AVR3a. New Phytologist **190**: 653-666.

**Gleave, A.P.** (1992). A versatile binary vector system with a T-DNA organisational structure conducive to efficient integration of cloned DNA into the plant genome. Plant Molecular Biology **20**: 1203-1207.

**Haas, B.J., Kamoun, S., Zody, M.C., Jiang, R.H.Y., Handsaker, R.E., Cano, L.M., Grabherr, M., Kodira, C.D., Raffaele, S., Torto-Alalibo, T., et al.** (2009). Genome sequence and analysis of the Irish potato famine pathogen *Phytophthora infestans*. Nature **461**: 393-398.

**Harding, M.W., Galat, A., Uehling, D.E., and Schreiber, S.L. (**1989). A receptor for the immunosuppressant FK506 is a *cis-trans* peptidyl-prolyl isomerase. Nature **341**: 758-760.

**Harrar, Y., Bellini, C., and Faure, J.-D.** (2001). FKBPs: at the crossroads of folding and transduction. Trends in Plant Science **6**: 426-431.

**Howell, S.H.** (2013). Endoplasmic reticulum stress responses in plants. Annual Review of Plant Biolog **64**: 477-499.

**Hausbeck, M.K., and Lamour, K.H.** (2004). *Phytophthora capsici* on vegetable crops: research progress and management challenges. Plant Disease **88**: 1292-1303.

**He, Z., Li, L., and Luan, S.** (2004). Immunophilins and parvulins: superfamily of peptidyl prolyl isomerases in Arabidopsis. Plant Physiology **134**: 1248-1267.

**Jansen, G., Määttänen, P., Denisov, A.Y., Scarffe, L., Schade, B., Balghi, H., Dejgaard, K., Chen, L.Y., Muller, W.J., Gehring, K., et al.** (2012). An interaction map of endoplasmic reticulum chaperones and foldases. Molecular and Cellular Proteomics **11**: 710-723.

**Jing, M., Guo, B., Li, H., Yang, B., Wang, H., Kong, G., Zhao, Y., Xu, H., Wang, Y., Ye, W., et al.** (2016). A *Phytophthora sojae* effector suppresses endoplasmic reticulum

stress-mediated immunity by stabilizing plant Binding immunoglobulin Proteins. Nature Communications **7**: 11685.

**Jiang, R.H.Y., Tripathy, S., Govers, F., and Tyler, B.M.** (2008). RXLR effector reservoir in two *Phytophthora* species is dominated by a single rapidly evolving superfamily with more than 700 members. Proceedings of the National Academy of Sciences USA **105**: 4874–4879.

**Jones, J.D., and Dangl, J.L.** (2006). The plant immune system. Nature **444**: 323-329.

**Kørner, C., Du, X., Vollmer, M., and Pajerowska-Mukhtar, K.** (2015). Endoplasmic reticulum stress signaling in plant immunity—at the crossroad of life and death. International Journal of Molecular Sciences **16**: 25964.

**Kale, S.D., Gu, B., Capelluto, D.G.S., Dou, D., Feldman, E., Rumore, A., Arredondo, F.D., Hanlon, R., Fudal, I., Rouxel, T., et al.** (2010). External lipid PI3P mediates entry of eukaryotic pathogen effectors into plant and animal host cells. Cell **142**: 284-295.

**Kamoun, S., Furzer, O., Jones, J.D.G., Judelson, H.S., Ali, G.S., Dalio, R.J.D., Roy, S.G., Schena, L., Zambounis, A., Panabières, F. et al.** (2015). The Top 10 oomycete pathogens in molecular plant pathology. Molecular Plant Pathology **16**: 413-434.

**Kazan, K., and Lyons, R.** (2014). Intervention of phytohormone pathways by pathogen effectors. Plant Cell **26**: 2285-2309.

**Kong, G., Zhao, Y., Jing, M., Huang, J., Yang, J., Xia, Y., Kong, L., Ye, W., Xiong, Q., Qiao, Y., et al.** (2015). The activation of *phytophthora* effector Avr3b by plant cyclophilin is required for the nudix hydrolase activity of Avr3b. PLoS Pathogens **11**: e1005139.

**King, S.R.F., McLellan, H., Boevink, P.C., Armstrong, M.R., Bukharova, T., Sukarta, O., Win, J., Kamoun, S., Birch, P.R.J., and Banfield, M.J.** (2014). *Phytophthora infestans* RXLR effector PexRD2 interacts with host MAPKKKε to suppress plant immune signaling. Plant Cell **26**: 1345-1359.

**Lamour, K.H., Mudge, J., Gobena, D., Hurtado-Gonzales, O.P., Schmutz, J., Kuo, A., Miller, N.A., Rice, B.J., Raffaele, S., Cano, L.M., et al.** (2012). Genome sequencing and mapping reveal loss of heterozygosity as a mechanism for rapid adaptation in the vegetable pathogen *Phytophthora capsici*. Molecular Plant-Microbe Interactions **25**: 1350-1360.

**Lang, K., Schmid, F.X., and Fischer, G.** (1987). Catalysis of protein folding by prolyl

isomerase. Nature **329**: 268-270.

**Li, J., Zhao-Hui, C., Batoux, M., Nekrasov, V., Roux, M., Chinchilla, D., Zipfel, C., and Jones J.D.** (2009). Specific ER quality control components required for biogenesis of the plant innate immune receptor EFR. Proceedings of the National Academy of Sciences USA **106**: 15973-15978.

**Liu, J.X., and Howell, S.H.** (2010). Endoplasmic reticulum protein quality control and its relationship to environmental stress responses in plants. Plant Cell **22**: 2930-2942.

**Llorente, B., Bravo-Almonacid, F., Cvitanich, C., Orlowska, E., Torres, H.N., Flawia, M.M., and Alonso, G.D.** (2010). A quantitative real-time PCR method for in planta monitoring of *Phytophthora infestans* growth. Letters in Applied Microbiology **51**: 603–610.

**Luan, S., Kudla, J., Gruissem, W., and Schreiber, S.L.** (1996). Molecular characterization of a FKBP-type immunophilin from higher plants. Proceedings of the National Academy of Sciences USA **93**: 6964-6969.

**Lucke, C., and Weiwad, M.** (2011). Insights into immunophilin structure and function. Current Medicinal Chemistry **18**: 5333-5354.

**McLellan, H., Boevink, P.C., Armstrong, M.R., Pritchard, L., Gomez, S., Morales, J., Whisson, S.C., Beynon, J.L., and Birch, P.R.J.** (2013). An RxLR Effector from *Phytophthora infestans* prevents re-localisation of two plant NAC transcription factors from the endoplasmic reticulum to the nucleus. PLoS Pathogens **9**: e1003670.

**Moreno, A.A., Mukhtar, M.S., Blanco, F., Boatwright, J.L., Moreno, I., Jordan, M.R., Chen, Y., Brandizzi, F., Dong, X., Orellana, A., et al.** (2012). IRE1/bZIP60-mediated unfolded protein response plays distinct roles in plant immunity and abiotic stress responses. PLoS ONE **7**: e31944.

**Nelson, B.K, Cai, X., and Nebenfuhr, A.** (2007). A multicolored set of in vivo organelle markers for co-localization studies in Arabidopsis and other plants. Plant Journal **51**: 1126-1136.

**Nekrasov, V., Li J., Batoux, M., Roux, M., Chu, Z.H., Lacombe, S., Rougon, A., Bittel, P., Kiss-Papp, M., Chinchilla, D., et al.** (2009). Control of the pattern-recognition receptor EFR by an ER protein complex in plant immunity. The EMBO Journal **28**: 3428-3438.

**Pan, Q., Cui, B., Deng, F., Quan, J., Loake, G.J., and Shan, W.** (2016). *RTP1* encodes a novel endoplasmic reticulum (ER)-localized protein in Arabidopsis and negatively regulates resistance against biotrophic pathogens. New Phytologist **209**: 1641-1654.

**Partaledis, J.A., and Berlin, V.** (1993). The FKB2 gene of *Saccharomyces cerevisiae*, encoding the immunosuppressant-binding protein FKBP-13, is regulated in response to accumulation of unfolded proteins in the endoplasmic reticulum. Proceedings of the National Academy of Sciences USA **90**: 5450-5454.

**Pogorelko, G.V., Mokryakova, M., Fursova, O.V., Abdeeva, I., Piruzian, E.S., and Bruskin, S.A.** (2014). Characterization of three *Arabidopsis thaliana* immunophilin genes involved in the plant defense response against *Pseudomonas syringae*. Gene **538**: 12-22.

**Qiang, X., Zechmann, B., Reitz, M.U., Kogel, K.-H., and Schäfer, P.** (2012). The mutualistic fungus piriformospora indica colonizes Arabidopsis roots by inducing an endoplasmic reticulum stress–triggered caspase-dependent cell death. Plant Cell **24**: 794-809.

**Qiao, Y., Liu, L., Xiong, Q., Flores, C., Wong, J., Shi, J., Wang, X., Liu, X., Xiang, Q., Jiang, S., et al.** (2013). Oomycete pathogens encode RNA silencing suppressors. Nature Genetics **45**: 330-333.

**Qiao, Y., Shi, J., Zhai, Y., Hou, Y., and Ma, W.** (2015). *Phytophthora* effector targets a novel component of small RNA pathway in plants to promote infection. Proceedings of the National Academy of Sciences USA **112**: 5850-5855.

**Rehmany, A.P., Gordon, A., Rose, L.E., Allen, R.L., Armstrong, M.R., Whisson, S.C., Kamoun, S., Tyler, B.M., Birch, P.R.J, and Beynon, J.L.** (2005). Differential recognition of highly divergent downy mildew avirulence gene alleles by *RPP1* resistance genes from two Arabidopsis lines. Plant Cell **17**: 1839-1850.

**Romano, P., Gray, J., Horton, P., and Luan, S.** (2005). Plant immunophilins: functional versatility beyond protein maturation. New Phytologist **166**: 753-769.

**Shan, W.X., Cao, M., Leung, D., and Tyler, B.M.** (2004). The Avr1b locus of *Phytophthora sojae* encodes an elicitor and a regulator required for avirulence on soybean plants carrying resistance gene Rps1b. Molecular Plant-Microbe Interactions **17**: 394–403.

**Turnbull, D., Yang, L., Naqvi, S., Breen, S., Welsh, L., Stephens, J., Morris, J., Boevink,**

**P.C., Hedley, P.E., Zhan, J., et al.** (2017). RXLR effector AVR2 up-regulates a brassinosteroid responsive bHLH transcription factor to suppress immunity. Plant Physiology **174**: 356-369.

**Tyler, B.M., Tripathy, S., Zhang, X., Dehal, P., Jiang, R.H., Aerts, A., Arredondo, F.D., Baxter, L., Bensasson, D., Beynon, J.L., et al.** 2006. *Phytophthora* genome sequences uncover evolutionary origins and mechanisms of pathogenesis. Science **313**: 1261-1266.

**Uknes, S., Dincher, S., Friedrich, L., Negrotto, D., Williams, S., Thompson-taylor, H., Potter, S., Ward, E., and Ryals, J.** (1993). Regulation of pathogenesis-related protein-1a gene-expression in tobacco. Plant Cell **5**: 159–169.

**Vasudevan, D., Gopalan, G., Kumar, A., Garcia, V.J., Luan, S., and Swaminathan, K.** (2015). Plant immunophilins: a review of their structure-function relationship. Biochimica et Biophysica Acta **1850**: 2145-2158.

**Vega-Arreguin, J. C., Jalloh, A. S., Bos, J. I. B., Moffett, P.** (2014). Recognition of an Avr3a homologue plays a major role in mediating nonhost resistance to *Phytophthora capsici* in *Nicotiana* species. Molecular Plant-Microbe Interactions **27**: 770-780.

**Wakasa, Y., Oono, Y., Yazawa, T., Hayashi, S., Ozawa, K., Handa, H., Matsumoto, T., and Takaiwa, F.** (2014). RNA sequencing-mediated transcriptome analysis of rice plants in endoplasmic reticulum stress conditions. BMC Plant Biology **14**: 101.

**Wang, D., Weaver, N.D., Kesarwani, M., and Dong, X.** (2005). Induction of protein secretory pathway is required for systemic acquired resistance. Science **308**: 1036-1040.

**Wang, S., Boevink, P.C., Welsh, L., Zhang, R., Whisson, S.C., and Birch, P.R.J.** (2017). Delivery of cytoplasmic and apoplastic effectors from *Phytophthora infestans* haustoria by distinct secretion pathways. New Phytologist **216**: 205-215.

**Wang, X., Boevink, P., McLellan, H., Armstrong, M., Bukharova, T., Qin, Z., and Birch, P.R.J.** (2015). A host KH RNA-binding protein is a susceptibility factor targeted by an RXLR effector to promote late blight disease. Molecular Plant **8**: 1385-1395.

**Wang, Y., Bouwmeester, K., Mortel, J.E.V.D., Shan, W., and Govers, F.** (2013). A novel Arabidopsis–oomycete pathosystem: differential interactions with *Phytophthora capsic*i reveal a role for camalexin, indole glucosinolates and salicylic acid in defence. Plant Cell and Environment **36**: 1192-1203.

**Wang, Y., Meng, Y., Zhang, M., Tong, X., Wang, Q., Sun, Y., Quan, J., Govers, F., and Shan, W.** (2011). Infection of *Arabidopsis thaliana* by *Phytophthora parasitica* and identification of variation in host specificity. Molecular Plant Pathology **12**: 187-201.

**Wawra, S., Trusch, F., Matena, A., Apostolakis, K., Linne, U., Zhukov, I., Stanek, J., Koźmiński, W., Davidson, I., Secombes, C., et al.** (2017). The RxLR motif of the host targeting effector AVR3a of *Phytophthora infestans* is cleaved before secretion. Plant Cell **29**: 1184-1195.

**Win, J., Kamoun, S., and Jones, A.E.** (2011). Purification of effector–target protein complexes via transient expression in *Nicotiana benthamiana*. In: Plant Immunity--McDowell, J.M. edited, Humana Press: 181-194.

**Wesley, S.V., Helliwell, C.A., Smith, N.A., Wang, M., Rouse, D.T., Liu, Q., Gooding, P.S., Singh, S.P., Abbott, D., Stoutjesdijk, P.A., et al.** (2001). Construct design for efficient, effective and high-throughput gene silencing in plants. Plant Journal **27**: 581-590.

**Whisson, S.C., Boevink, P.C., Moleleki, L., Avrova, A.O., Morales, J.G., Gilroy, E.M., Armstrong, M.R., Grouffaud, S., West, P.V., Chapman, S., et al.** (2007). A translocation signal for delivery of oomycete effector proteins into host plant cells. Nature **450**: 115-118.

**Yang, L., McLellan, H., Naqvi, S., He, Q., Boevink, P.C., Armstrong, M., Giuliani, L.M., Zhang, W., Tian, Z., Zhan, J., et al.** (2016). Potato NPH3/RPT2-like protein StNRL1, targeted by a *Phytophthora infestans* RXLR effector, is a susceptibility factor. Plant Physiology **171**: 645-657.

**Yun, B.W., Atkinson, H.A., Gaborit, C., Greenland, A., Read, N.D., Pallas, J.A., and Loake, G.J.** (2003). Loss of actin cytoskeletal function and EDS1 activity, in combination, severely compromises non-host resistance in Arabidopsis against wheat powdery mildew. Plant Journal **34**: 768–777.

**Zhang, X., Henriques, R., Lin, S.S., Niu, Q.W., and Chua, N.H.** (2006). Agrobacterium-mediated transformation of *Arabidopsis thaliana* using the floral dip method. Nature Protocols **1**: 641-646.

## FIGURES AND FIGURE LEGENDS

**Figure 1. *P. capsici* RXLR Effector PcAvr3a12 is a Virulence Factor.**

**(A)** Expression of *PcAvr3a12* at different infection stages was determined by quantitative RT-PCR. Four-week-old leaves from *A. thaliana* Col-0 were inoculated with *P. capsici* zoospores. Total RNA was extracted from mycelia and infected leaves at 3, 6, 12, 24, 36, 48 and 60 hour post inoculation (hpi). *P. capsici* actin gene (Gene ID: jgi|Phyca11|132086) was used as internal control. Error bars indicate standard deviation (SD) of three biological replicates.

**(B)** Transgenic *A. thaliana* lines constitutively expressing *FLAG-PcAvr3a12* showed

enhanced susceptibility to *P. capsici* infection. Image was taken at 60 hpi.

**(C)** *P. capsici* colonization at 60 hpi was determined by quantitative PCR. Primers specific for *P. capsici* actin gene and *A. thaliana UBC9* gene (Gene ID: AT4G27960) were used. Error bars indicate SD of four biological replicates, with at least eight leaves per replicate.

**(D)** Immunoblotting using anti-FLAG antibody to detect effector protein expression. Two independent transgenic *A. thaliana* lines expressing *FLAG-PcAvr3a12* and one *FLAG-GFP* expressing *A. thaliana* line were examined.

**Figure 2. Identification of the Host Protein AtFKBP15-2 Interaction with *P. capsici* RXLR Effector PcAvr3a12.**

**(A)** Y2H assays showing that PcAvr3a12 specifically interacts with AtFKBP15-2. Yeast strain AH109 co-expressing empty bait vector (BD) or bait vector containing *PcAvr3a12*, *PiAvr3a*$^{KI}$ or *PcAvr3a14* and empty prey vector (AD) or prey vector containing *AtFKBP15-2*, *AtFKBP15-1* or *PcFKBP35* were grown on auxotrophic media (SD/-Leu-Trp) with about $10^5$ cells (left panel). Only yeast cells co-expressing *PcAvr3a12* and *AtFKBP15-2* grew on auxotrophic media (SD/-Leu-Trp-His) (middle panel) and yielded β-galactosidase (β-Gal) activity (right panel), while other yeast cells did not. ΔAtFKBP15-2 and ΔAtFKBP15-1 represent specific protein constructs in which the signal peptide and the potential ER retention signal were truncated, respectively. Three independent experiments showed consistent results.

**(B)** Domain architectures of AtFKBP15-2 and AtFKBP15-1.

**(C)** The bait/prey swap experiments in Y2H assays confirmed that PcAvr3a12 specifically interacts with AtFKBP15-2. Yeast cells co-expressing *PcAvr3a12* with *FKBP15-2* grew on auxotrophic media (SD/-Leu-Trp-His-Ade), whereas the control pairs did not. Three independent experiments showed consistent results.

**(D)** Co-immunoprecipitation assays showing that PcAvr3a12 interacts with AtFKBP15-2 *in planta*. Total native protein extracts (Input) from agroinfiltrated leaves expressing the indicated protein complexes precipitated with GFP-Trap agarose beads (IP: GFP), were separated on SDS-PAGE gels and blotted with specific antibodies. For the input fraction a similar amount of 7*myc-PcAvr3a12 with SP-GFP-FKBP15-2 was used. In

immunoprecipitation fractions, 7*myc-PcAvr3a12 was only detected in the complex with SP-GFP-FKBP15-2-NDEL but not with FLAG-GFP or the empty vector. Protein size markers were indicated in kDa, and protein loading was indicated by ponceau staining. The experiments were repeated twice with similar results.

**Figure 3. *FKBP15-2* Positively Regulates *A. thaliana* Resistance to *Phytophthora* pathogens.**

**(A-B)** Expression of *FKBP15-2* at different stages during *P. capsici* or *P. parasitica* infection was determined by quantitative RT-PCR. Four-week-old leaves from Col-0 were inoculated with *P. capsici* zoospores (A). Total RNA was extracted from infected leaves at 0, 3, 6, 12, 24, 36, 48 and 60 hpi. Two-week-old roots of Col-0 were infected with zoospores from *P. parasitica* (B). Total RNA was extracted from infected roots at 0, 6, 12, 24, 48 and 60 hpi. *A. thaliana UBC9* was used as internal control. Error bars indicate SD of three biological replicates.

**(C)** The expression of *FKBP15-2* in the T-DNA insertion mutant *fkbp15-2* and the WT Col-0 as determined by real-time RT-PCR. Total RNA was extracted from leaves of the 4-week-old plant leaves. *UBC9* was used as internal control. Error bars indicate SD of three biological replicates.

**(D, F)** Detached leaf inoculation assays showing that *fkbp-15-2* is susceptible to *P. capsici* (D) and *P. parasitica* (F). Image was taken at 60 hpi (D) and 72 hpi (F).

**(E, G)** *P. capsici* or *P. paracitica* colonization of infected leaves at 60 or 72 hpi as determined by qPCR. Primers specific for *P. capsici* actin gene, *P. parasitica UBC* gene (Gene ID: PPTG_08273) and *A. thaliana UBC9* gene were used. Error bars indicate SD of three biological replicates, with at least 8 leaves per replicate.

**(H)** *P. capsici* biomass in infected leaves of FKBP15-2-OE-19, FKBP15-2-OE-24, FKBP15-2-RNAi-8, FKBP15-2-RNAi-9 lines and Col-0 at 60 hpi was determined by real-time PCR. Error bars indicate SD of three biological replicates, with at least 8 leaves per replicate.

**(I)** *P. parasitica* colonization of infected *A. thaliana* roots. Total genomic DNA from *P. parasitica* infected roots was isolated at 48 hpi. Error bars indicate SD of three biological

946 replicates, with 24 seedling roots per replicate.

947

948 **Figure 4. *P. capsici* RXLR Effector PcAvr3a12 Associates with the Host Protein**
949 **FKBP15-2 at the Endoplasmic Reticulum.** Proteins were expressed in *N. benthamiana*
950 leaves through agroinfiltration with *Agrobacterium tumefaciens* cell suspension at $OD_{600}$
951 value of 0.3. Fluorescence was observed by confocal microscopy at 48 hour post
952 agroinfiltration in *N. benthamiana* epidermal cells. Fluorescence plots show the relative
953 fluorescence along the dotted line in the images.
954 **(A)** SP-GFP-FKBP15-2-NDEL fluorescence overlaps with the mCherry labeled ER-marker at
955 the peri-nuclear ER (upper panel) and the ER network (lower panel). Scale bar, 20 µm.
956 **(B)** SP-mCherry-FKBP15-2-NDEL fluorescence partially overlaps with GFP-PcAvr3a12 at
957 the peri-nuclear ER (upper panel) and the ER network (lower panel). In the lower panel,
958 agroinfiltration with *Agrobacterium tumefaciens* cell suspension at $OD_{600}$ value of 0.1. Scale
959 bar, 20 µm.
960 **(C-E)** The association of PcAvr3a12 and FKBP15-2 in living cells was detected by
961 bimolecular fluorescence complementation (BiFC). The C-terminus of Venus (VC) was fused
962 to the N-terminus of PcAvr3a12 and $PiAvr3a^{KI}$ (mature protein with signal peptide deleted)
963 and the N-terminus of Venus (VN) was fused between the secretory signal peptide and
964 FKBP15-2-NDEL or FKBP15-1-KNEL. Co-expression of SP-VN-FKBP15-2-NDEL and
965 VC-PcAvr3a12 resulted in specific fluorescence as detected by confocal microscopy (C), in
966 contrast to two control combinations (D-E). Scale bar, 40µm. Three independent experiments
967 showed similar results.
968 **(F)** Enlarged image shows a representative fluorescent cell expressing
969 SP-VN-FKBP15-2-NDEL and VC-PcAvr3a12. Scale bar, 20µm.
970 **(G)** A quantitative statistical analysis for the average number of fluorescent cells per
971 observable field using 20x magnification and identical settings for each of the replicates.
972 Significantly more fluorescent cells were observed *SP-VN-FKBP15-2-NDEL* and
973 *VC-PcAvr3a12* co-expression as compared to control combinations ($p < 0.001$, t test, $n = 12$
974 fields of view for each couple).

**Figure 5. *P. capsici* Effector PcAvr3a12 and Host Protein FKBP15-2 Accumulate Around Haustoria During *Phytophthora* Infection.** Each construct was expressed in *N. benthamiana* leaves through agroinfiltration with *Agrobacterium tumefaciens* cell suspension ($OD_{600}$ of 0.2 to 0.3). Infiltrated leaves were inoculated with *P. capsici* or GFP-expressing *P. parasitica* zoospores at 24 hour post agroinfiltration. Fluorescence was observed by confocal microscopy at 60 hour post agroinfiltration. GFP and mCherry signals are indicated in green and red, respectively. White arrows indicate *Phytophthora* haustoria. The fluorescence plots show the relative fluorescence along the dotted line in the images. Scale bars, 10 µm. Three independent biological replicates showed similar results.

**(A)** Fluorescence of SP-mCherry-FKBP15-2-NDEL indicates its accumulation around haustoria during infection by GFP-labeled *P. parasitica*.

**(B)** Fluorescence of ER-marker indicates the ER-embraced haustoria during infection by GFP-labeled *P. parasitica*.

**(C)** Fluorescence of mCherry-PcAvr3a12 indicates its accumulation around haustoria during infection by GFP-labeled *P. parasitica*.

**(D)** GFP-PcAvr3a12 and SP-mCherry-FKBP15-2-NDEL co-localized around haustoria following inoculation with *P. capsici*.

**(E)** Localization of GFP-PcAvr3a12 and mCherry-PiAvrblb2 around haustoria following infection with *P. capsici*.

**Figure 6. PPIase Activity of FKBP15-2 is Required for Its Immune Function to *Phytophthora*.**

**(A)** PPIase activity of FKBP15-2 and FKBP15-$2^{D93A}$. The recombinant proteins MBP-GFP, MBP-ΔFKBP15-2 and MBP-ΔFKBP15-$2^{D93A}$ were expressed and purified from *E. coli*. The "Δ" indicated specific protein constructs in which the signal peptide and the potential ER

retention signal were truncated. PPIase activities were analyzed by chymotrypsin-coupled assay using succinyl-Ala-Leu-Pro-Phe-p-nitroanilide as substrate at 8 $^{o}$C. A faster absorbance peak at 390 nm is indicative for higher PPIase activity. The final concentration of each purified protein in the mix was 10 μM. The MBP-GFP was used as a control. Three independent replicates showed similar results.

**(B)** PPIase activity assay for MBP-ΔFKBP15-2, combined with PcAvr3a14, rapamycin or PcAvr3a12. The recombinant proteins MBP-FKBP15-2, MBP-PcAvr3a12 and MBP-PcAvr3a14 were expressed and purified from *E. coli*. Rapamycin is a chemical suppressor of PPIases. MBP-PcAvr3a14 and rapamycin were used as controls. The final concentration of each purified protein in the mix, including MBP-FKBP15-2, MBP-PcAvr3a12 and MBP-PcAvr3a14, was 10 μM. PPIase activity was analyzed by chymotrypsin-coupled assay using succinyl-Ala-Leu-Pro-Phe-p-nitroanilide as substrate at 8 $^{o}$C. A faster absorbance peak at 390 nm is indicative for higher PPIase activity. Three independent experiments showed similar results.

**(C)** Detached leaves of *FKBP15-2* mutant complementation lines ($CM^{D93A}$) showing enhanced susceptibility to infection by *P. capsici* zoospores. Representative image was taken at 60 hpi.

**(D)** *P. capsici* biomass in infected leaves of Col-0, *FKBP15-2* complementation lines (CM) and its mutant complementation lines ($CM^{D93A}$) at 60 hpi, as determined by qPCR. Error bars indicate SD from three biological replicates.

**(E)** Protein stability of FKBP15-2, co-expressed with PcAvr3a12 or mCherry, were analyzed by immunoblotting. The SP-GFP-FKBP15-2-NDEL was co-expressed with FLAG-PcAvr3a12 or mCherry in *N. benthamiana* leaves through agroinfiltration. Total proteins were extracted from infiltrated leaves at 1, 2 and 3 day/s post agroinfiltration. The SP-GFP-FKBP15-2-NDEL and FLAG-PcAvr3a12 were detected by immunoblotting using anti GFP- and FLAG-antibodies, respectively. Ponceau staining of the membrane to show equal loading.

**Figure 7. *FKBP15-2* is Involved in UPR and ER stress-Mediated Plant Immunity to *Phytophthora*.**

**(A)** The dynamic expressions of *bZIP60*, *bZIP28*, *BiP3* and spliced *bZIP60* were measured by real-time RT-PCR. 10-day-old seedlings of WT Col-0 and *fkbp15-2* mutants were sprayed with TM (5 μg/mL). The total RNA was extracted from seedlings at 0, 3, 6 and 12 hours post treatment. *UBC9* was used as plant reference gene. Error bars indicate SD from three biological replicates. Asterisks indicate significant differences ($P < 0.05$).

**(B)** Expression levels of *bZIP60*, *bZIP28*, *γVPE*, *WRKY33*, *CYP81F2* and *EFR* were determined by real-time RT-PCR. Detached leaves of the 4-week-old plants of WT Col-0 and *fkbp15-2* mutants were inoculated with *P. capsici* zoospores. Total RNA was extracted from leaves at 0, 3, 6 and 12 hpi. *UBC9* was used as plant reference gene. Error bars indicate SD of three biological replicates. Asterisks indicate significant differences ($P < 0.05$).

**(C)** Fresh weight of *fkbp15-2* and Col-0 under TM-triggered ER stress. 4-day-old WT Col-0 and *fkbp15-2* mutant seedlings were grown in liquid medium with TM (50 ng/ml), using DMSO as a negative control. Seedling fresh weight was determined at 7 days post treatment. For each sample, at least 12 seedlings were used. Three independent experiments showed similar results. Error bars indicate SD from twelve seedlings. Asterisks indicate significant differences ($P < 0.01$).

**Figure 8. A Schematic Model of the Role of FKBP15-2 and PcAvr3a12 in Plant Immunity to *Phytophthora*.**

*P. capsici* develops haustoria to secrete and deliver effectors, including PcAvr3a12, into host cells to manipulate host cell function. Plant ER-localized PPIase, FKBP15-2, accumulates and embraces around haustoria. FKBP15-2 is directly targeted and inhibited by PcAvr3a12 around haustoria. *Phytophthora* infection activates an ER stress response and ER stress-mediated immunity in plants. T-DNA insertion mutant *fkbp15-2* shows significant attenuation of *bZIP60* and *bZIP28* expression and of multiple ER-processed immune genes (e.g. *γVPE*, *EFR*, *WRKY33* and *PR1*). Based on these results, we propose that *P. capsici*-secreted RXLR effector PcAvr3a12 circumvents plant immunity by targeting and suppressing a novel ER -localized immune protein, FKBP15-2, which positively regulates plant resistance through participating in ER stress-mediated plant immunity. CW, cell wall; PM, plasma membrane; H, haustoria; ER, endoplasmic reticulum.

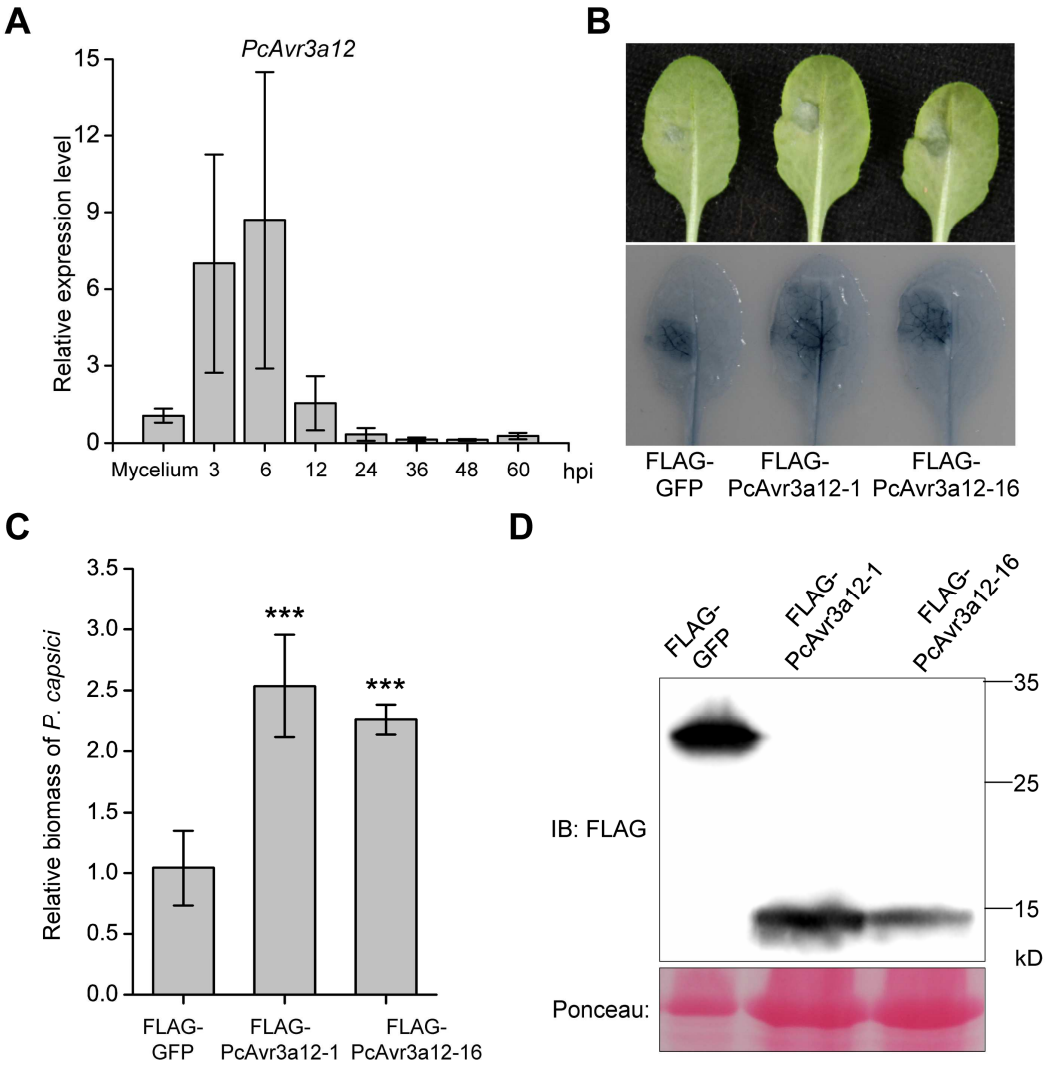
A
PcAvr3a12
Relative expression level
15
12
9
6
3
0
Mycelium 3 6 12 24 36 48 60 hpi
B
FLAG-GFP
FLAG-PcAvr3a12-1
FLAG-PcAvr3a12-16
C
Relative biomass of P. capsici
3.5
3.0
2.5
2.0
1.5
1.0
0.5
0.0
***
***
FLAG-GFP
FLAG-PcAvr3a12-1
FLAG-PcAvr3a12-16
D
FLAG-GFP
FLAG-PcAvr3a12-1
FLAG-PcAvr3a12-16
IB: FLAG
35
25
15
kD
Ponceau:

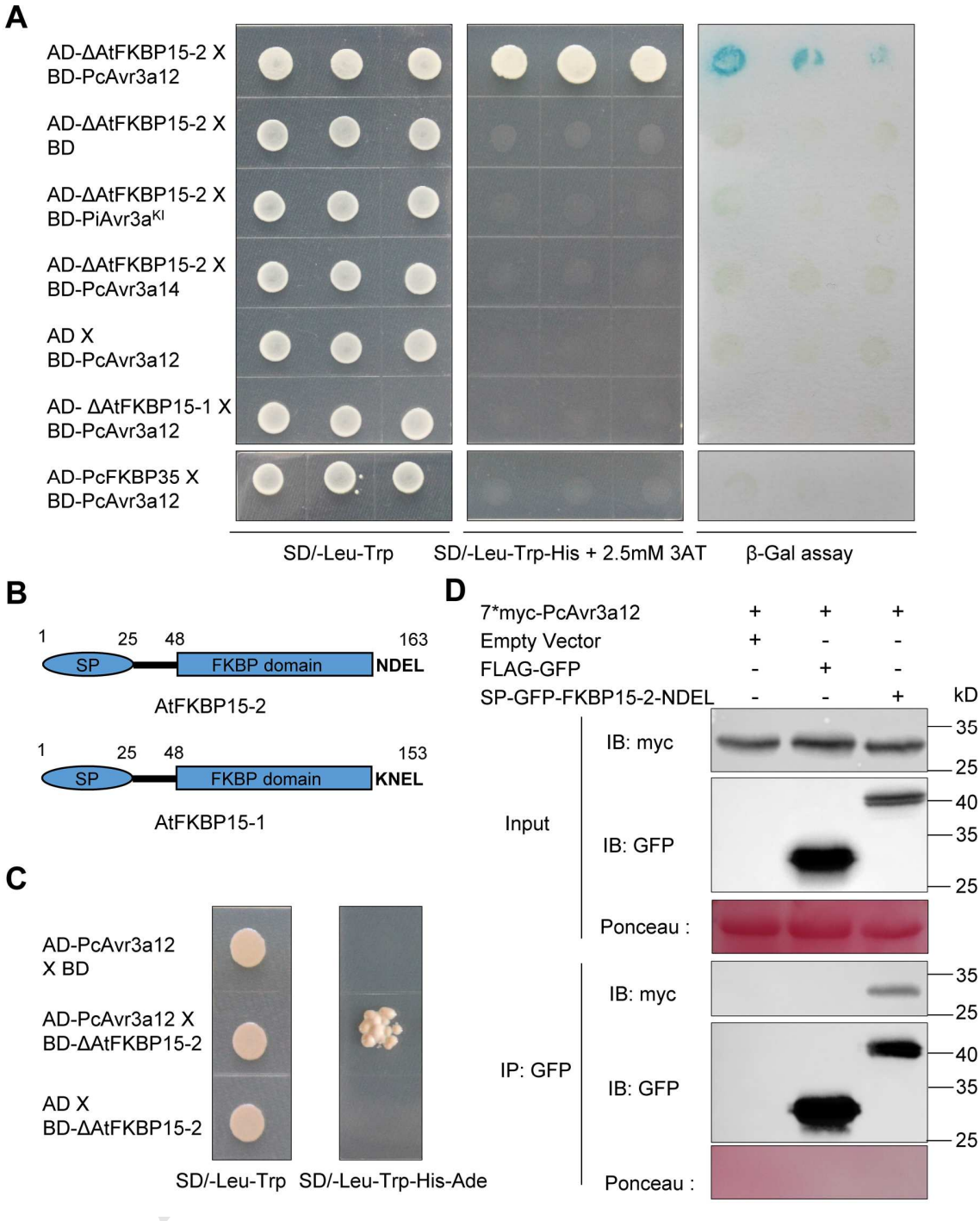
A
AD-ΔAtFKBP15-2 X BD-PcAvr3a12
AD-ΔAtFKBP15-2 X BD
AD-ΔAtFKBP15-2 X BD-PiAvr3a^KI
AD-ΔAtFKBP15-2 X BD-PcAvr3a14
AD X BD-PcAvr3a12
AD- ΔAtFKBP15-1 X BD-PcAvr3a12
AD-PcFKBP35 X BD-PcAvr3a12
SD/-Leu-Trp
SD/-Leu-Trp-His + 2.5mM 3AT
β-Gal assay
B
1
25
48
163
SP
FKBP domain
NDEL
AtFKBP15-2
1
25
48
153
SP
FKBP domain
KNEL
AtFKBP15-1
C
AD-PcAvr3a12 X BD
AD-PcAvr3a12 X BD-ΔAtFKBP15-2
AD X BD-ΔAtFKBP15-2
SD/-Leu-Trp
SD/-Leu-Trp-His-Ade
D
7*myc-PcAvr3a12 + + +
Empty Vector + - -
FLAG-GFP - + -
SP-GFP-FKBP15-2-NDEL - - +
kD
Input
IB: myc
IB: GFP
Ponceau :
IP: GFP
IB: myc
IB: GFP
Ponceau :
35
25
40
35
25
35
25
40
35
25

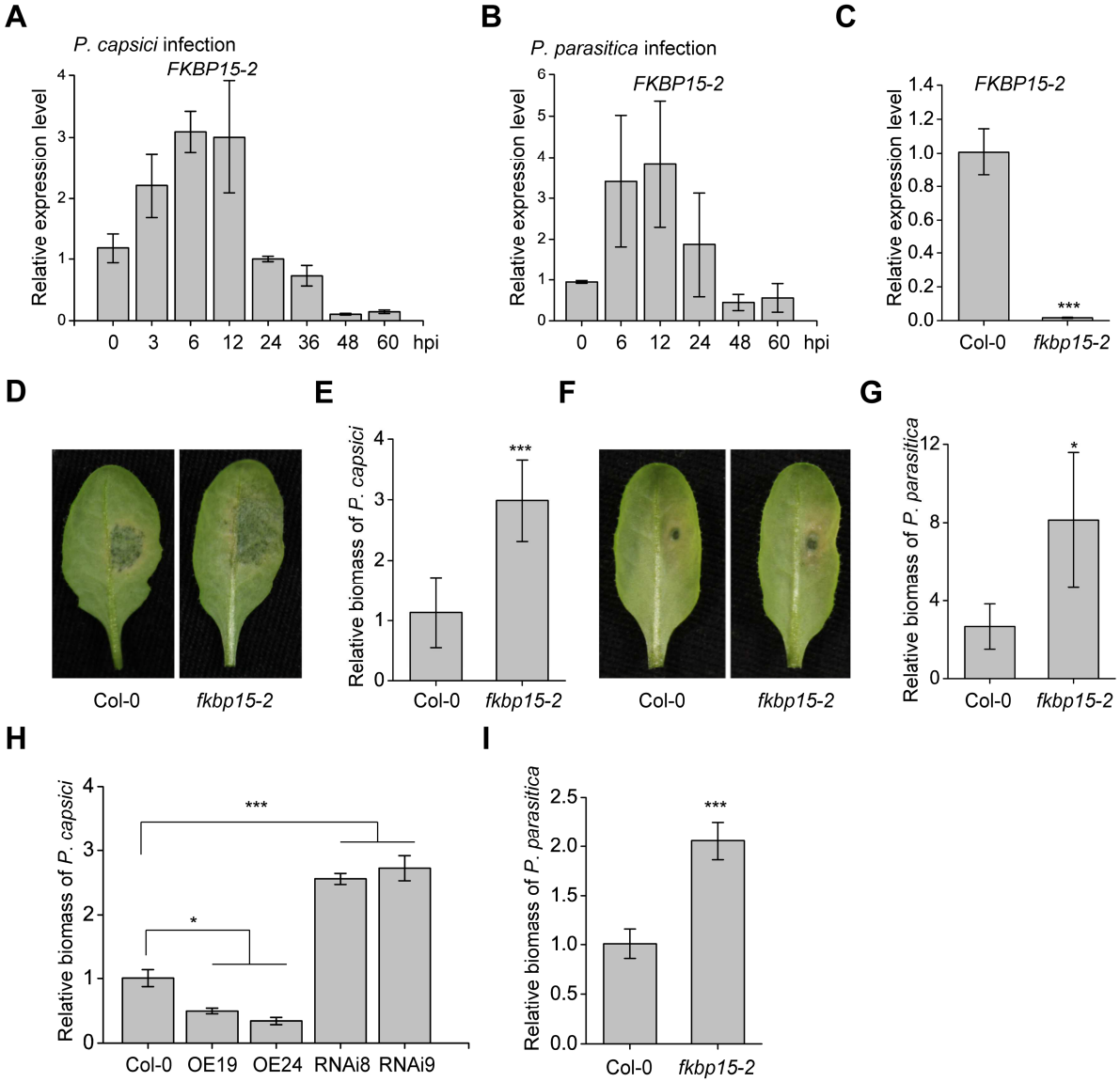
A
P. capsici infection
FKBP15-2
Relative expression level
0 3 6 12 24 36 48 60 hpi
B
P. parasitica infection
FKBP15-2
Relative expression level
0 6 12 24 48 60 hpi
C
FKBP15-2
Relative expression level
***
Col-0 fkbp15-2
D
Col-0 fkbp15-2
E
Relative biomass of P. capsici
***
Col-0 fkbp15-2
F
Col-0 fkbp15-2
G
Relative biomass of P. parasitica
*
Col-0 fkbp15-2
H
Relative biomass of P. capsici
***
*
Col-0 OE19 OE24 RNAi8 RNAi9
I
Relative biomass of P. parasitica
***
Col-0 fkbp15-2

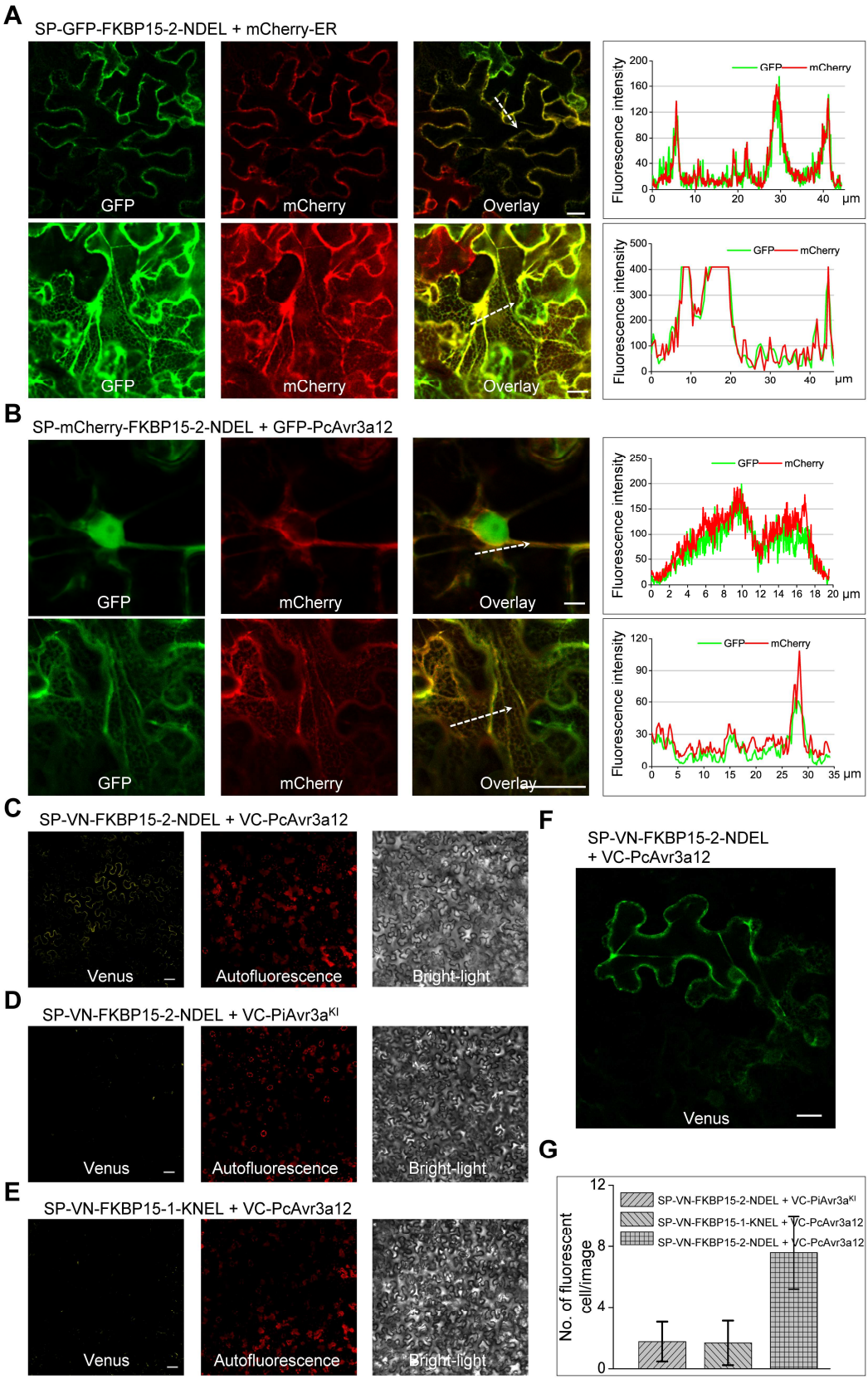
A
SP-GFP-FKBP15-2-NDEL + mCherry-ER
GFP
mCherry
Overlay
Fluorescence intensity
GFP
mCherry
μm
B
SP-mCherry-FKBP15-2-NDEL + GFP-PcAvr3a12
C
SP-VN-FKBP15-2-NDEL + VC-PcAvr3a12
Venus
Autofluorescence
Bright-light
D
SP-VN-FKBP15-2-NDEL + VC-PiAvr3a^KI
E
SP-VN-FKBP15-1-KNEL + VC-PcAvr3a12
F
SP-VN-FKBP15-2-NDEL
+ VC-PcAvr3a12
G
No. of fluorescent cell/image
SP-VN-FKBP15-2-NDEL + VC-PiAvr3a^KI
SP-VN-FKBP15-1-KNEL + VC-PcAvr3a12
SP-VN-FKBP15-2-NDEL + VC-PcAvr3a12

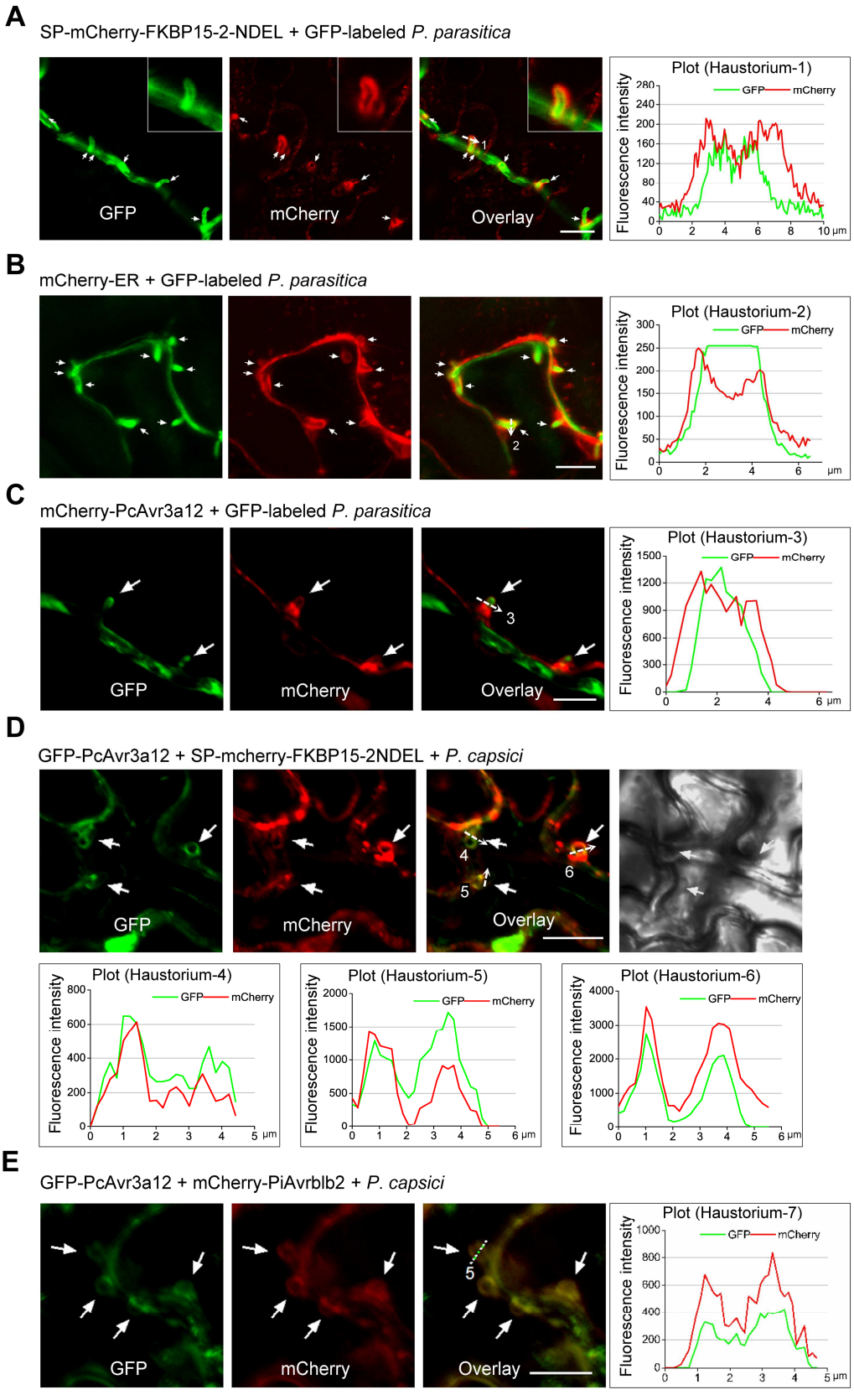
A
SP-mCherry-FKBP15-2-NDEL + GFP-labeled P. parasitica
GFP
mCherry
Overlay
Plot (Haustorium-1)
Fluorescence intensity
GFP
mCherry
B
mCherry-ER + GFP-labeled P. parasitica
Plot (Haustorium-2)
C
mCherry-PcAvr3a12 + GFP-labeled P. parasitica
Plot (Haustorium-3)
D
GFP-PcAvr3a12 + SP-mcherry-FKBP15-2NDEL + P. capsici
Plot (Haustorium-4)
Plot (Haustorium-5)
Plot (Haustorium-6)
E
GFP-PcAvr3a12 + mCherry-PiAvrblb2 + P. capsici
Plot (Haustorium-7)

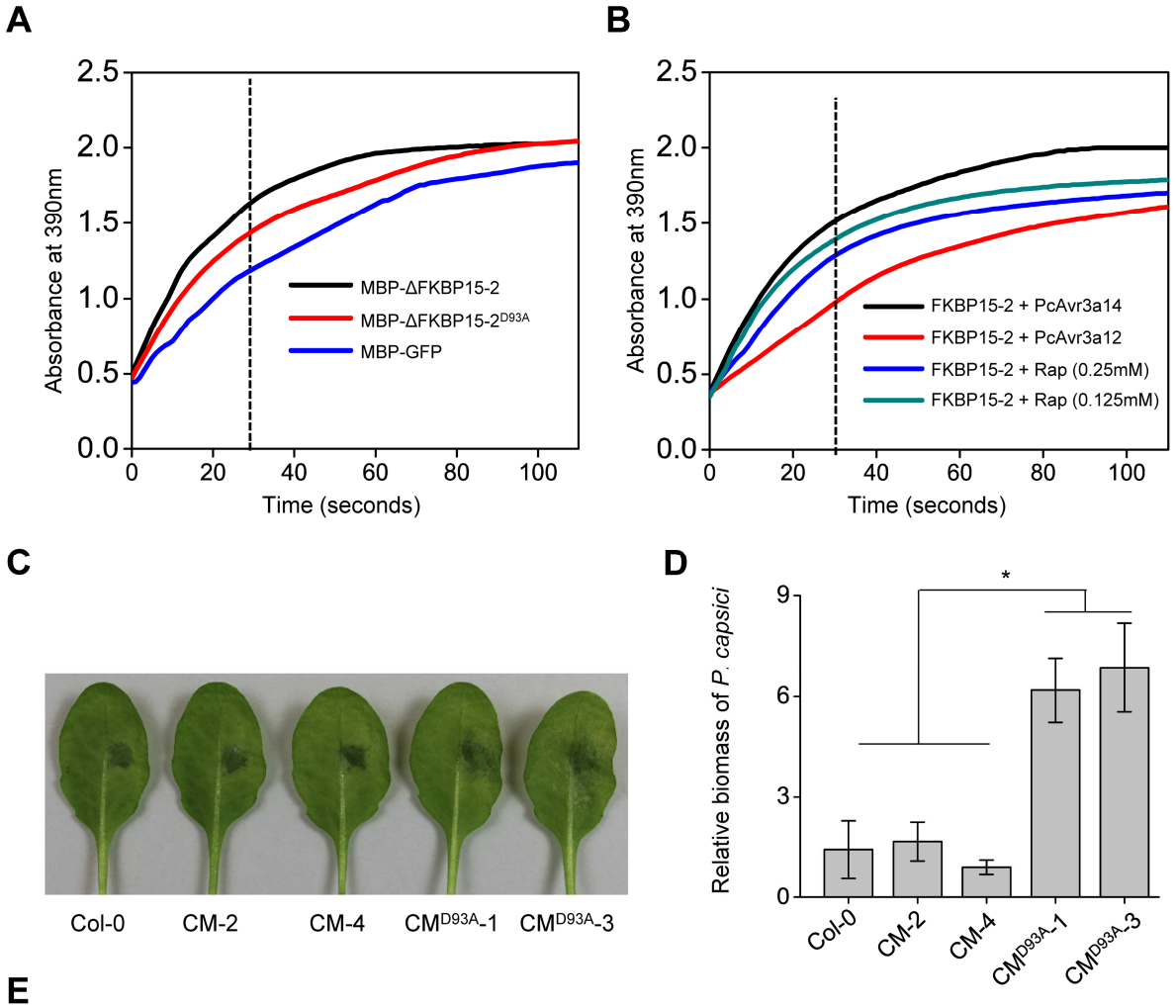
A
B
Absorbance at 390nm
Time (seconds)
MBP-ΔFKBP15-2
MBP-ΔFKBP15-2D93A
MBP-GFP
FKBP15-2 + PcAvr3a14
FKBP15-2 + PcAvr3a12
FKBP15-2 + Rap (0.25mM)
FKBP15-2 + Rap (0.125mM)
C
Col-0
CM-2
CM-4
CMD93A-1
CMD93A-3
D
Relative biomass of P. capsici
*
E
SP-GFP-FKBP15-2-NDEL
FLAG-PCAvr3a12
mCherry
kD
IB:GFP
IB:FLAG
Ponceau:
24
48
72
hour

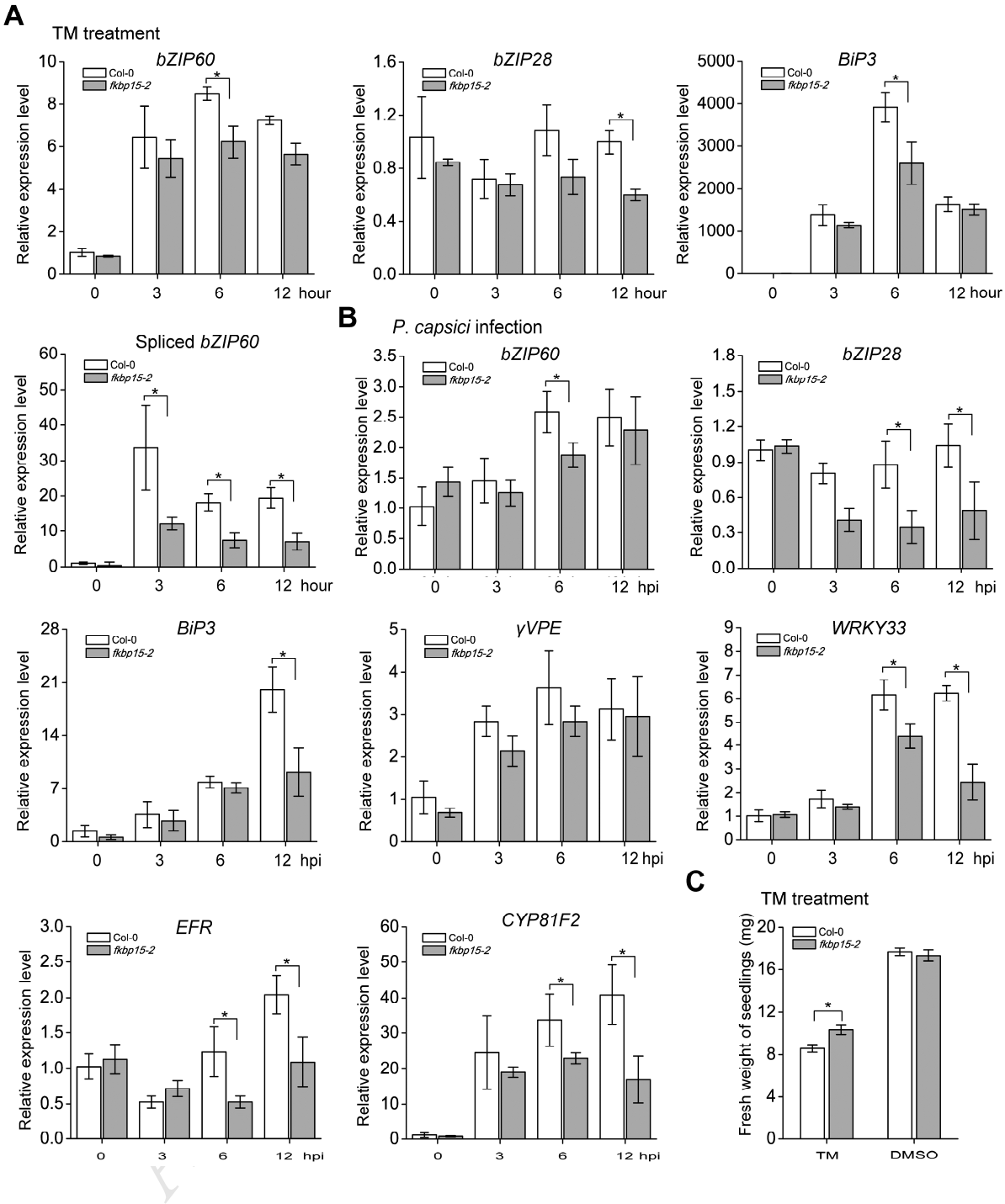
A
TM treatment
bZIP60
bZIP28
BiP3
Col-0
fkbp15-2
Relative expression level
0 3 6 12 hour
B
P. capsici infection
Spliced bZIP60
bZIP60
bZIP28
BiP3
γVPE
WRKY33
EFR
CYP81F2
0 3 6 12 hpi
C
TM treatment
Fresh weight of seedlings (mg)
TM
DMSO